JOINT WMO TECHNICAL PROGRESS REPORT ON THE GLOBAL DATA PROCESSING AND FORECASTING SYSTEM AND NUMERICAL WEATHER PREDICTION RESEARCH ACTIVITIES FOR 2015

Croatian Meteorological and Hydrological Service (DHMZ)

1. Summary of highlights

Work on the limited area model ALADIN focused mainly on migration of NWP system on new HPC and testing of new model version (cy38t1). Also coupling of ALADIN with ECMWF became operationally.

2. Equipment in use at the Centre

The computer used for the forecasting system is an SGI UV 2000 (Figure 1 and Table 1). The storage is Quantum Scalar i500 and the visualization is based on Grads, Magics, Metview, Python and R.

Table 1. *Computers used operationally.*

Computer	Memory	Storage
Model forecast: SGI UV 2000	608 GB	7.1 TB
Storage: Quantum Scalar i500	8 GB	32TB disc + tapes
Visualization: Linux server	125 GB	3.5 TB

Model forecast:

- SGI UV 2000
- 28 Intel Xeon E5 6core 2,9GHz 15MB cache CPUs with total 228 cores
- 608 GB RAM
- working disks 7.1TB
- Intel compilers version 13.1.0 20130121
- PBSPro, SGI management software, Fibre Channel, Gigabit Ethernet

Storage:

- Quantum Scalar i500
- OS SUSE Linux Enterprise Server 10 for IPF with SGI Package
- 32Tb online data + tapes

Main users: NWP, Air-quality modeling & Climate modeling

Figure 1. Operational computer system at DHMZ.

3. Data and Products from GTS in use

- SYNOP
- TEMP
- AMDAR
- SHIP
- FAX
- GRIB
- BUFR

4. Forecasting system

4.1 System run schedule and forecast ranges

The operational Limited Area Model ALADIN 8-km resolution forecast (HR88) is run four times per day (00, 06, 12, 18 UTC) for 72 hours ahead using lateral boundary conditions (LBC) from ECMWF global model in so-called *lagged mode*. Lagged mode is used because of time constrains for ALADIN forecast and times of availability of ECMWF forecast. In lagged mode there is 6 hours shift between initialization time of global model and HR88 model e.g. for HR88 forecast initialized at 00 UTC, ECMWF forecast initialized at 18 UTC is used for LBC. The 8-km resolution forecast are dynamically adapted to the 2 km resolution topography in a procedure (DADA) designed to improve high resolution wind forecast, especially in case of severe wind events. The procedure is performed for each output file of the 8-km resolution forecast with 1-hourly frequency. Parallel run of future operational ALADIN model with 4km horizontal grid spacing and 73 vertical levels (HR44) was set up from beginning of February 2015. HR44 is run once per day starting at 00 UTC and it is also coupled to ECMWF global model in lagged mode. The high-resolution ALADIN full model forecast at the 2-km resolution is run only once per day (HR22). The initial file is interpolated 6 hour forecast of the 8km resolution run that started at 00 UTC. The forecast range is 24 hours and covers the observing period of the rain gauges. Forecast ranges and product availability times are shown in Table 2.

Table 2. *The main features of the operational model runs.*

Suite	Initialization time	Initial conditions	LBC	Start time	End time	Products availability
ALADIN-8	00	Assimilation	ECMWF	02:55	03:25	03:30
ALADIN-8	06	Assimilation	ECMWF	08:55	09:25	09:30
ALADIN-8	12	Assimilation	ECMWF	14:55	15:25	15:30
ALADIN-8	18	Assimilation	ECMWF	20:55	21:25	21:30
ALADIN-2	06	ALARO-8 (00UTC)	ALARO-8 (00UTC)	03:00	03:31	03:35
ALADIN-4	00	Surface assimilation	ECMWF	04:10	05:10	05:15

4.2 Medium range forecasting system (4-10 days)

There are three global model products available. The IFS operational forecast output is available from ECMWF, GME from DWD and the ARPEGE model output is available from Meteo-France.

4.3 Short-range forecasting system (0-72 hrs)

The operational HR88 is run four times per day, initialized from local data assimilation cycle. The operational forecast is run 72 hours ahead on a Lambert-projection domain with 8 km horizontal resolution with 37 hybrid sigma-pressure levels in the vertical. From 1 January 2014 LBC from ECMWF are used operationally (Tudor et al 2015a).

The model forecast fields from 8km resolution run are subsequently going through a dynamical adaptation procedure (Ivatek-Šahdan and Tudor, 2004) that produces a 2-km resolution forecast of 10 m wind speed and gusts. The dynamical adaptation method of Žagar and Rakovec (1999) has been adapted for the purpose of operational forecast of the 10 m wind. The method provides successful operational forecast of the 10 m wind (Ivatek-Šahdan and Tudor, 2004) and is used extensively in research impact studies (Bajić et al., 2007) as well as case studies of severe wind (Tudor and Ivatek-Šahdan, 2002).

The model fields are first interpolated from the low resolution (8 km in this case) to a higher resolution (2 km) grid, but at a considerably lower number of model levels – at 15 out of 37 vertical levels. The number of vertical levels is reduced to minimize computational cost. The levels close to the ground are of similar density, and the higher levels are mostly omitted. Then a hydrostatic version of the ALADIN model is run for 30 time steps with a 60-second time step. The same large-scale model data are used as initial and boundary conditions, therefore the fields at lateral boundaries do not change during the adaptation procedure. Turbulence is the only parameterization scheme used. Contributions from the moist and radiation processes are not computed in order to accelerate the model integration.

As an addition to operational forecast, future operational forecast HR44 was set up in parallel suite. It uses LBC from ECMWF global model and it is initialized from data assimilation cycle with only surface data assimilation as a first step in preparing full data assimilation cycle. The model forecast

is calculated one per day (00 UTC) up to 72 hours ahead on a Lambert-projection domain with 4 km horizontal resolution with 73 hybrid sigma-pressure levels in the vertical.

Also 2-km resolution 24-hour forecast is performed once per day, with non-hydrostatic (NH) dynamics in the ALADIN model and the full parameterization set, including the convection scheme. This forecast is performed once per day, following the 00 UTC operational 8-km forecast. It uses the 6-hour forecast from the 8-km operational run as an initial file and is run with the Scale-Selective Digital Filter Initialization (SSDFI). This high-resolution forecast is then integrated for 24 hours, until 6 UTC on the next day. This procedure covers the 24-hour period allowing the collection of precipitation data from rain gauges.

4.3.1 Data assimilation, objective analysis and initialization

4.3.1.2. In operation

The assimilation system is operational from November 2011. It consists of two parts: surface assimilation, which is used to initialize the state of the modeled land surface variables, and the upper-air assimilation (Figure 2). Surface assimilation is made by the optimal interpolation (OI) technique, while the upper-air assimilation is conducted using the 3D Variational technique (3DVAR). Surface assimilation uses 2 m temperature and relative humidity observations. For upper-air assimilation the following observations are used: SYNOP, TEMP, AIREP, wind-profiler and measurements from polar and geostationary satellites (Table 3). Observational data is available through local exchange facility (OPLACE - Observation Pre-processing for LACE) installed and maintained in the Hungarian Meteorological Service in Budapest. In addition, the data-assimilation suite uses the data from the network of automatic stations of Croatia. More details about assimilation setup can be found in Stanešić (2011).

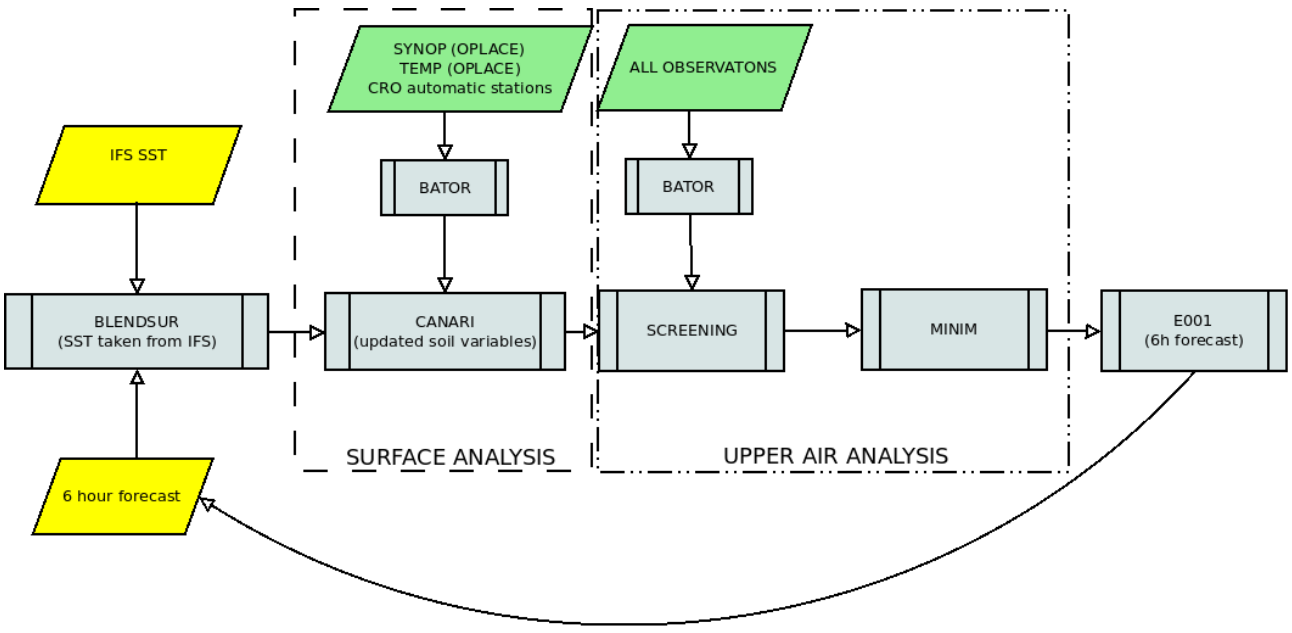

Figure 2. *Scheme of assimilation cycle at DHMZ.*

The forecast error is approximated by a set of forecast differences valid at the same verification time, but at different forecast ranges, the so-called standard NMC method of background error-matrix calculation. The method uses 100 forecast differences from the period 15 February until 25

May 2008. The model runs are initialized with a 24-hour time difference and the forecast ranges (36h and 12h forecasts) used for the B-matrix calculation were valid at 00 UTC. The B matrix is isotropic in the horizontal and follows a multivariate formulation of vorticity, divergence, temperature and surface pressure and specific humidity as the control variables. The operational B matrix is currently not tuned.

Analysis cycle is executed four times per day using a long cut-off observational data and LBCs. At the beginning of 6-hour forecast inside assimilation cycle, digital filter initialization (DFI; Lynch, 1997) is applied. Similar procedure is done for the production, only difference is that a short cut-off data and LBCs are used and at the end 72-hour forecast is performed.

Data assimilation cycle for HR88 model performs both surface and upper air analysis while for HR44 model only surface data assimilation was set up as a first step (upper air analysis will be added subsequently). No DFI is used in HR44 data assimilation cycle.

For the 2-km resolution run a SSDFI is used to initialize the fields, since the usual DFI removes some meteorological high resolution features from the initial model fields (Termonia, 2008).

Table 3. *Observations used in the operational 3DVAR assimilation system.*

Observation system	Assimilated fields
SYNOP	T2m,RH2m,Φ
SHIP	T2m,RH2m,Φ,U10m,V10m
AMDAR/AIRREP	U,V,T
TEMP	U,V,T,Q, Φ
WINDPROFILER	U,V
GEOWIND	U,V
NOAA 16, 18 (AMSUA, AMSUB, MHS)	radiance
MSG SEVIRI	radiance

4.3.2 Model

4.3.2.1 In operation

The model system for the short range weather forecast used at Meteorological and Hydrological Service (DHMZ) is ALADIN. The same integration domain for 8-km resolution run (HR88) and 4-km resolution run (HR44) is used and it is shown in Figure 3 and the domain for the 2-km resolution run (HR22) is shown in Figure 4. The main characteristics of the operational forecast model (see Tudor et al 2015a) are listed in Table 4.

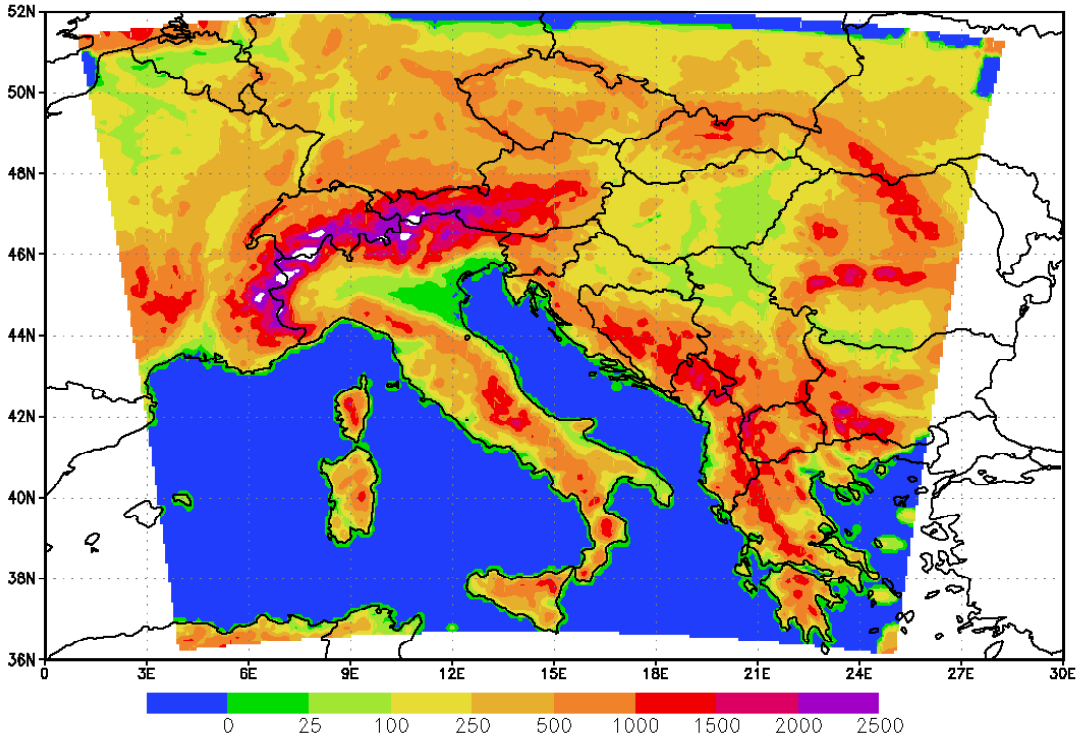

Figure 3. *Domain and model topography (shaded, in meters) of ALADIN-Croatia 8 km resolution run, 11 rows on the northern edge and 11 columns on the eastern edge are the extension zone.*

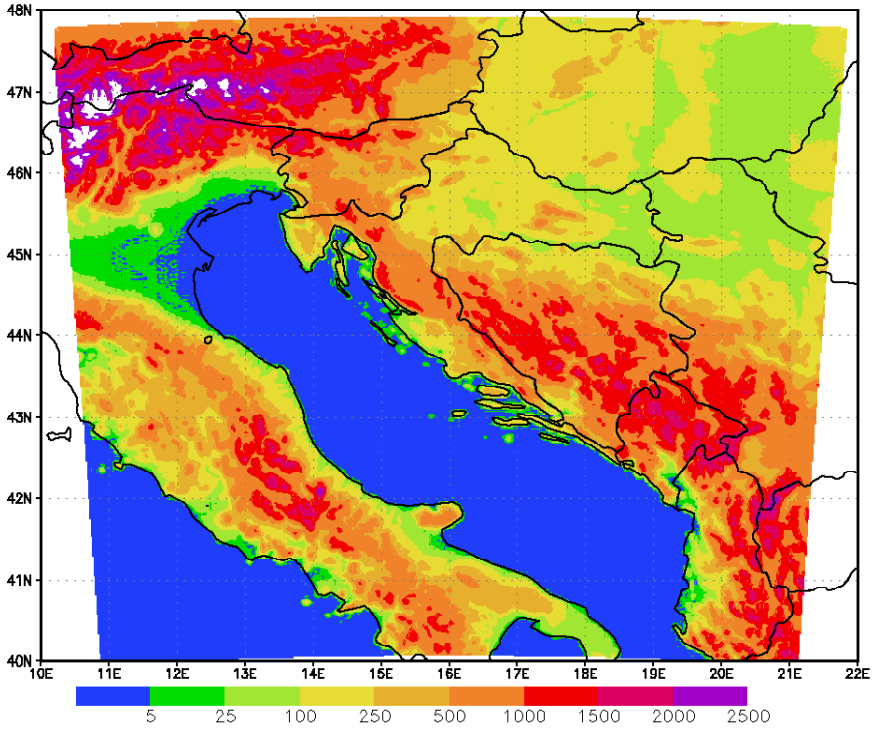

Figure 4. *Domain and model topography (shaded, in meters) of ALADIN-Croatia 2km resolution non-hydrostatic run and high-resolution dynamical adaptation.*

Horizontal diffusion in NWP models is employed to suppress the accumulation of energy at the shortest wavelengths. In ALADIN this used to be achieved by a common 4^{th} order numerical diffusion at the end of each time step. The semi-Lagrangian horizontal diffusion (SLHD) is computed by combining two semi-Lagrangian interpolators of different diffusivity with the flow deformation as a weighting factor. This procedure yields an improved horizontal diffusion scheme that is based on the physical properties of the flow (Vana et al., 2008). The SLHD is used in parallel model versions since December 2006 and it is fully operational since February 2008.

The ALARO0 physics parameterization package includes prognostic schemes for turbulence, microphysics and convection. The turbulent exchange coefficients are computed using prognostic values of turbulent kinetic energy (TKE) according to Geleyn et al. (2006). Contribution of shallow convection is computed using the moist turbulence scheme from Geleyn 1988.

The parameterization scheme for land surface, Interaction Soil Biosphere Atmosphere (ISBA; Noilhan and Planton, 1989), is used in operational forecast as well as in the surface data assimilation (Giard and Bazile, 2000).

Cloud microphysics describes the processes of condensation, evaporation, freezing and melting as well as the processes that transform the cloud water droplets and ice crystals into rain and snow. A simple microphysics scheme is used with prognostic cloud water and ice, rain and snow (Catry et al., 2007) and a statistical approach for sedimentation of precipitation (Geleyn et al., 2008).

Table 4. *Model characteristics in different model runs.*

	ALADIN 8km	**ALADIN 4 km**	**2km HRDA**	**2km NH**
Horizontal resolution	8 km	4 km	2 km	2 km
Spectral truncation	(quadratic) 79x71	(quadratic) 159x143	(quadratic) 149x149	(quadratic) 149x149
Number of levels	37	73	15	37
Number of grid points	240x216	480x432	450x450	450x450
Time step (sec)	327.273	180	60	60
Forecast range (hrs)	72	72	72	24
Initialization	OI + 3Dvar	OI	No	SSDFI
Coupling model	ARPEGE or IFS	IFS	ALADIN 8km	ALADIN 8km
Coupling freq. (hrs)	3 (Davies relaxation)	3 (Davies relaxation)	constant LBCs, (Davies relax.)	1 (Davies relaxation)
Output frequency (hrs)	1 and 3	1 and 3	1 and 3	1
Dynamics	Hydrostatic, 2 time level, semi implicit, semi lagrangian	Hydrostatic, 2 time level, semi implicit, semi lagrangian	Hydrostatic, 2 time level, semi implicit, semi lagrangian	non-hydrostatic, 2 time level, semi implicit, semi lagrangian

	ALADIN 8km	ALADIN 4 km	2km HRDA	2km NH
Orography	Mean	Mean	mean	mean
Grid (gp and spec)	A, quadratic	A, quadratic	A, quadratic	A, quadratic
Physics	ALARO0	ALARO0	Turbulence only	ALARO0
Horizontal diffusion	SLHD	SLHD	SLHD	SLHD

The convective processes redistribute momentum, heat and moisture in the vertical. Within ALARO0 physics package, there is modular multi-scale micro-physics and transport (3MT) scheme for precipitation and clouds (Gerard and Geleyn, 2005; Gerard, 2007; Gerard et al., 2009). The scheme uses prognostic variables for up-draft and down-draft vertical velocities and mesh fractions, entrainment and convective clouds. The 3MT scheme is operational since January 2015.

The processes of condensation, evaporation, freezing, melting, aggregation and growth of cloud water and ice into rain and snow are described by the micro-physics. Prognostic scheme for the cloud water and ice, rain and snow and a statistical approach for sedimentation of precipitation (Geleyn et al., 2008) is derived upon the old diagnostic scheme based on the Kessler (1969) type scheme with modifications (Geleyn et. al. 1994). The scheme is re-tuned in order to avoid fibrillations that occur due to a combination of melting and sublimation parameters (Tudor, 2013).

The transfer, scattering, absorption and reflection of the short-wave solar radiation and long-wave thermal radiation of the Earth's surface and clouds are parameterized in radiation scheme (Geleyn and Hollingsworth, 1979, Ritter and Geleyn, 1982). The scheme uses only one spectral band for long-wave and one for short-wave radiation. The net exchange rate has been introduced in the scheme (Geleyn et. al. 2005a, 2005b) and recently switched on in the operational forecast set-up. This radiation scheme is computationally cheap, so the computations are done each model time-step, avoiding possible numerical instability (Pauluis and Emmanuel, 2004).

The vertical transfer of heat, momentum and moisture due to impact of the unresolved motion and surface roughness are described by turbulence parameterization that uses prognostic turbulent kinetic energy (TKE) that is advected, diffused (Geleyn et al., 2006) combined with modified Louis (1979) dependency on stability (Redelsperger et al., 2001). The contribution of the shallow convection to the evolution of model variables is computed in the turbulence scheme (Geleyn, 1987).

Wind, temperature and humidity are interpolated from the model levels to the standard meteorological measurement heights (10 and 2 meters above surface) using a parameterized profile (Geleyn, 1988).

4.3.2.2 Research performed in this field

Problems with fast storms and long coupling update intervals

Three-hourly temporal resolution of lateral boundary data for limited area models (LAMs) can be too infrequent to resolve rapidly moving storms (Tudor and Termonia, 2010). This problem is expected to be worse with increasing horizontal resolution. In order to detect intensive disturbances

in surface pressure moving rapidly through the model domain, a filtered surface pressure field (MCUF) is computed operationally in the ARPEGE global model of Météo France. The field is distributed in the coupling files along with conventional meteorological fields used for lateral boundary conditions (LBCs) for the operational forecast using limited area model ALADIN (Aire Limitée Adaptation dynamique Développement InterNational) in the Meteorological and Hydrological Service of Croatia (DHMZ). An analysis is performed of the MCUF field for the LACE coupling domain (Tudor, 2015) for the period from 23 January 2006, when it became available, until 15 November 2014. The MCUF field is a good indicator of rapidly moving pressure disturbances (RMPDs). Its spatial and temporal distribution can be associated with the usual cyclone tracks and areas known to be supporting cyclogenesis. An alternative set of coupling files from the IFS operational run in the European Centre for Medium-Range Weather Forecasts (ECMWF) is also available operationally in DHMZ with 3-hourly temporal resolution, but the MCUF field is not available. Several methods are tested that detect RMPDs in surface pressure a posteriori from the IFS model fields provided in the coupling files (Tudor, 2015). MCUF is computed by running ALADIN on the coupling files from IFS. The error function is computed using one-time-step integration of ALADIN on the coupling files without initialization, initialized with digital filter initialization (DFI) or scale-selective DFI (SSDFI). Finally, the amplitude of changes in the mean sea level pressure is computed from the fields in the coupling files. The results are compared to the MCUF field of ARPEGE and the results of same methods applied to the coupling files from ARPEGE. Most methods give a signal for the RMPDs, but DFI reduces the storms too much to be detected. The error functions without filtering and amplitude have more noise, but the signal of a RMPD is also stronger.

Implementation of wave model forecast

In order to provide forecast of height and direction of wind waves, model has been ported and set up to perform daily runs. The Wind Wave Model (WWM) is an unstructured grid spectral wave model. It incorporates most existing source term formulation for wind input and dissipation. It uses residual distribution schemes for the horizontal advection. It integrates the wave action equation (WAE) by using the operator splitting method in explicit or implicit mode.

The WWM model was set up to use the wind output from the ALADIN model. Model runs for 36 hours starting at 0000 UTC, limited by the available wave model data. Runtime is 20 minutes on 66 processors. Time step is 5 minutes for the implicit scheme. Figures are automatically created both for the whole Adriatic and for the Istrian region. The model is run with boundary data at the Otranto strait obtained from the global WAM model. This is what limits us to 36 hours of simulation starting at 0000 UTC. Model data is interpolated in time, space and spectrum to the boundary. Other alternative would have been to use WW3 IFREMER data, but this is from a commercial service.

A faster implicit solver has been developed. We solve the linear system Ax=b by the Jacobi method. Solution technique is to iterate. Most of the computational time is spent for the solver part. The number of iterations is about 30. What happens is that most of the action in the solver happens at a few places in the grid. Thus by discarding points which have converged and will not change, we speed up the convergence process.

Validation of HR44 model

The experiments were performed in which a set of 31 forecasts up to 72 hours in advance were run starting from 00 UTC initial files for each day in January and May 2014 (Tudor et al. 2015b). The standard scores of forecasts in 4 km resolution are superior to the 8 km forecast. The results on 73

levels show improved forecast of 2 m temperature and relative humidity for May, but worse forecast of relative humidity and temperature at 2 meters in January (***Figure 5***). The introduction of non-hydrostatic dynamics did not show substantial impact to the standard scores when computed for one whole month. The brief summary of the results for several experiments is given in Table 3. The operational suite currently assimilates surface data through optimum interpolation, while 3D-var is to be implemented once the background error covariance matrix is computed.

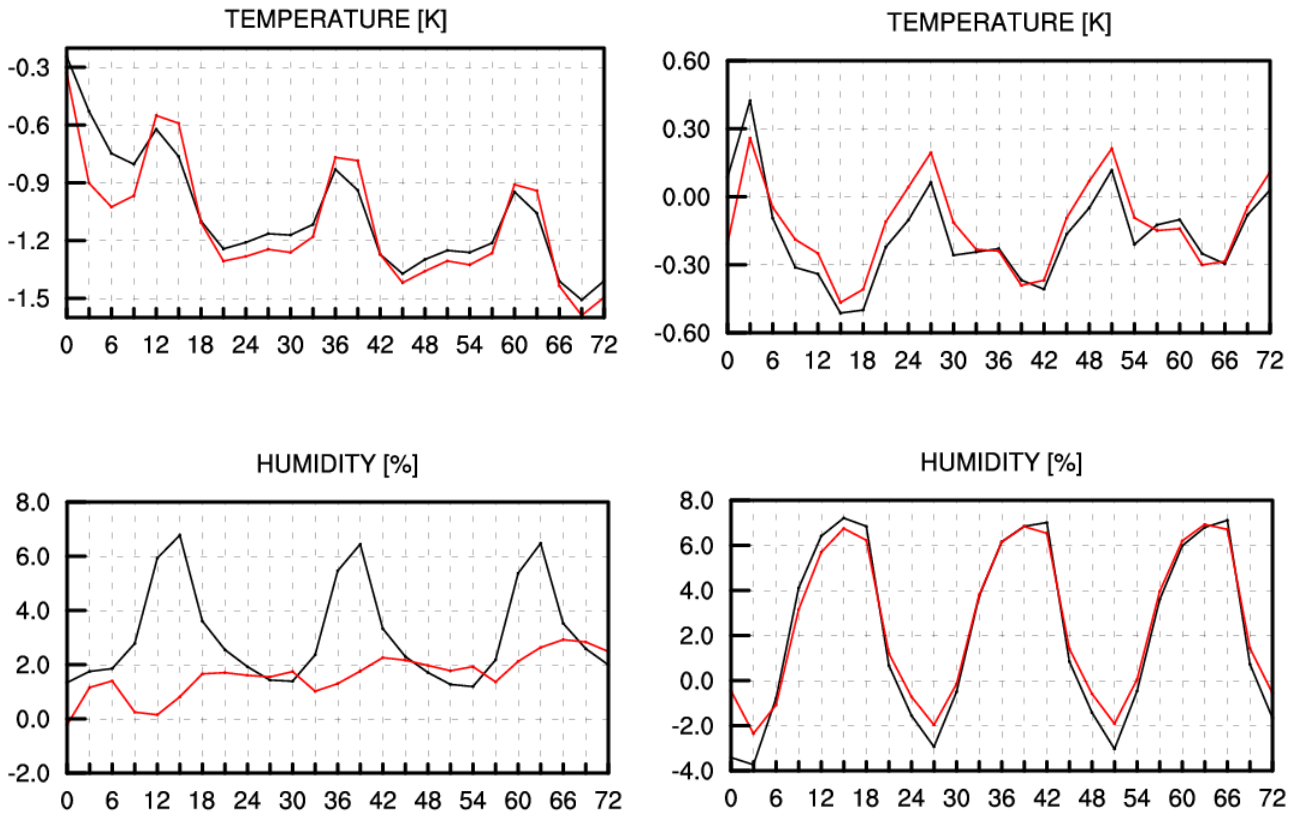

Figure 5. *Bias computed for the 4 km resolution forecast (black) and 8 km (red) using ALARO0 for 2 m temperature dependency on forecast time (from 0 to 72 hours) for 31 forecasts starting from 00 UTC during January (a) and May (b) 2014*

Other models

The WRF models is being run in research mode for specific research purposes at the research department for the last ten years, such as case studies of extreme winds in complex terrain, convection and heavy precipitation, internal gravity waves, meteotsunamis, near-surface wind shear, and other. Various setups are currently tested, including varying grid spacing, PBL parametrizations, convection schemes, microphysics schemes, type of nesting etc. Current tests focused on high-resolution modelling of wind speed variability in very complex terrain of the eastern Adriatic coast and comparing of results we achieved for the western US. The grid spacing used in this study reached grid spacing of 333 m and assessed the ability of the model to simulate wind variability on the order of seconds. The simulations used ECWMF operational analysis for initial and lateral boundary conditions. Further tests are planned using the WRF model with LES closure instead of PBL parametrization, as well as testing several subfilter parametrizations.

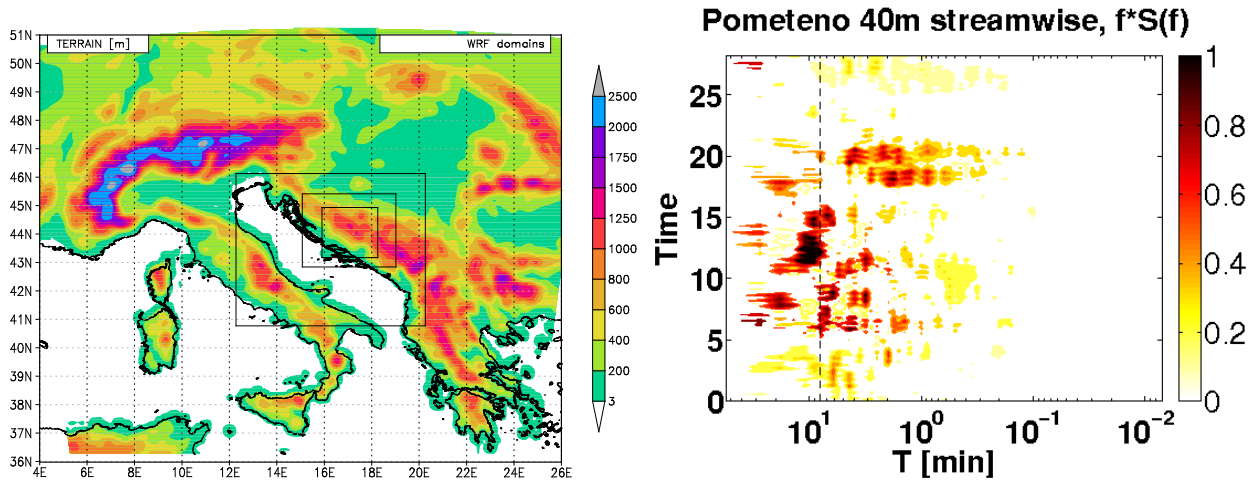

***Figure 6**. Left: WRF domains for mid-Adriatic Bora test case on 28 Apr 2010 at 9 km, 3 km, 1 km and 333 m grid spacing. Right: Spectral decomposition of WRF wind speed at location Pometeno brdo.*

4.3.3 Operationally available NWP products

Output variables of the 8km resolution run (3 hourly outputs):

- 3D: u, v, omega (Pa/s), geopotential, vorticity, divergence, absolute and potential vorticity, temperature, potential and equipotential temperature and relative moisture on pressure levels (1000, 975, 950, 925, 900, 850, 800, 700, 600, 500, 300, 250 hPa);
- 2D: u, v 10m above ground, temperature and relative humidity 2m above ground, low, medium, high and convective cloudiness, stratiform and convective rain and snow, mean sea level pressure, wind gusts u and v components, CAPE, moisture convergence, PBL height, and the Showalter, Sweat, k-index and totals-totals (in)stability indices,
- 2D: pre-defined vertical cross sections of wind, temperature, humidity, potential temperature, vertical velocity, TKE and snow.

Output variables of the HR88 and HR44 model (1 hourly output):

- 3D: model output fields used for initial and LBCs of the 2km resolution model runs
- values at approximately 300 pre-defined model points of mean sea level pressure, cloudiness (low, medium, high, convective), precipitation (rain and snow), 2m temperature and humidity, 10m wind speed, direction and gusts used for meteograms,
- upper level values of potential temperature, humidity, wind speed and direction used for the high-resolution isentropic analysis (HRID).

Output variables of the 2km resolution dynamical adaptation of the wind field:

- 10m wind speed, direction and gusts figures are produced 3 hourly, data are hourly,
- Wind speed and direction at 80m for locations of wind farms (Figure 7)
- pre-defined vertical cross-sections of potential temperature wind speed and direction.

Output variables of the 2km resolution non-hydrostatic forecast (hourly outputs):

- 3D: u, v, omega (Pa/s), geopotential, potential vorticity, potential temperature and relative humidity on pressure levels (1000, 975, 950, 925, 900, 850, 800, 700, 600, 500, 300, 250 hPa);
- 2D: u, v 10m above ground, temperature and relative humidity 2m above ground, low, medium, high and convective cloudiness, stratiform and convective rain and snow, mean sea level pressure, wind gusts u and v components, CAPE, moisture convergence PBL height, and the Showalter, Sweat, k-index and totals-totals (in)stability indices.

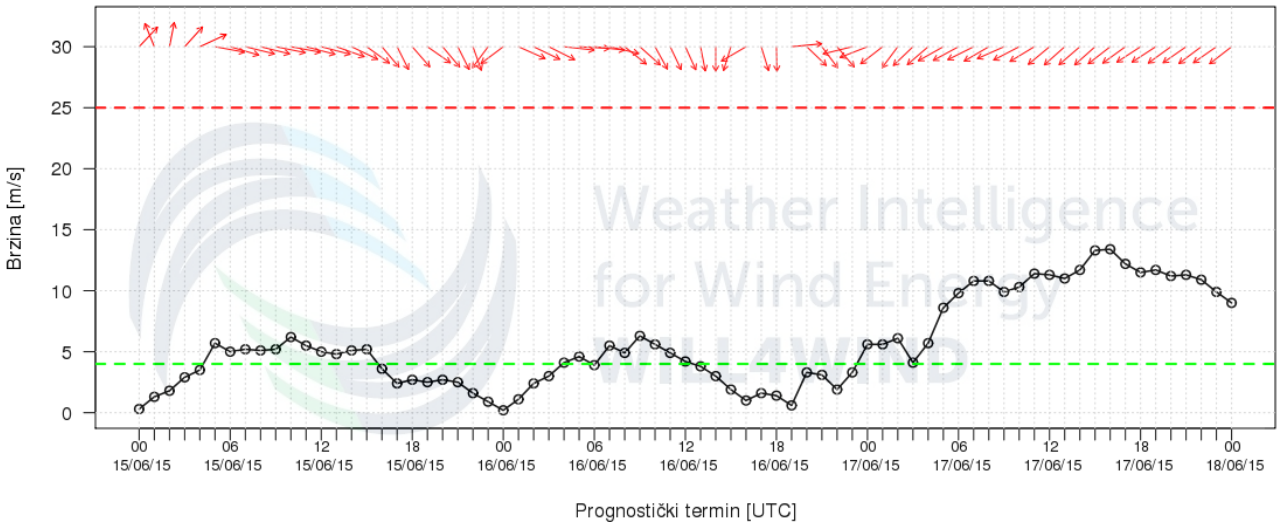

Figure 7. *Wind speed and direction at 80m at location of one wind farm. On x axis forecast hour in UTC is given, while on y axis wind speed in m/s is shown. Wind direction is indicated by red arrows.*

4.3.4 Operational techniques for application of NWP products (MOS, PPM, KF, Expert Systems etc.)

4.3.4.1 In operation

4.3.4.2 Research performed in this field

Two probabilistic forecasts produced using the same dataset and training period are compared for the probabilistic prediction of wind speed exceeding 5 ms^{-1} (relatively rare event): logistic regression approach (LR) and analog-based technique (AnEn). The predictions were generated by ALADIN run over two nested domain with 8 and 2 km horizontal resolution, respectively, as well as by an operational 2 km-resolution dynamical adaptation model and tested at several climatologically different locations across Croatia for point-based wind speed predictions at 10 m height. Results are shown for ALADIN 8 km model and all the available locations. Statistical consistency measures (spread diagram and rank histogram) are only possible for the ensemble (AnEn) forecasts, so these results are not compared to LR.
The AnEn forecasting seems to be somewhat more reliable than LR, although both of them exhibit a good degree of reliability (**Figure 8**). For the smallest forecast probabilities (0-0.2 bin), both methods provide a slight overestimation of the observed relative frequency. Above that value, AnEn slightly overestimates, while LR underestimates the observed relative frequency. The forecast relative frequency for every bin reveals good tendency to predict extreme probabilities, with the majority occurring in the 0.0 - 0.2 probability range. The AnEn and LR forecasts are similarly sharp, except for AnEn (LR) predicts the highest (smallest) forecast probability been a bit more often. Combined with good reliability, this is a trustworthy sharpness (i.e., does not result in overconfidence). The LR forecasting is somewhat more reliable for greater lead times than AnEn, but that is likely due to the low probability class that is close to climatological forecasting (not shown).

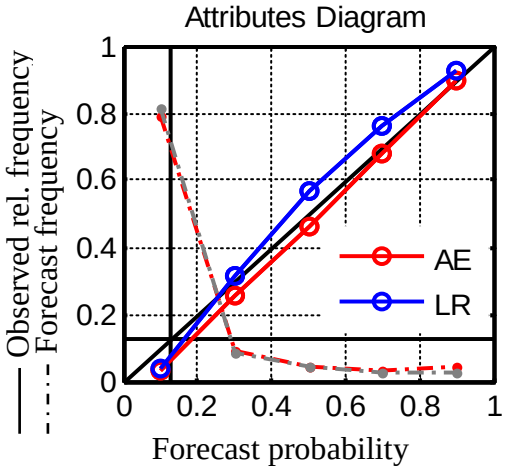

Figure 8. The attributes diagram of AnEn and LR probabilistic prediction of 10-m wind speed greater than 5 ms^{-1} at 14 locations during 2012.

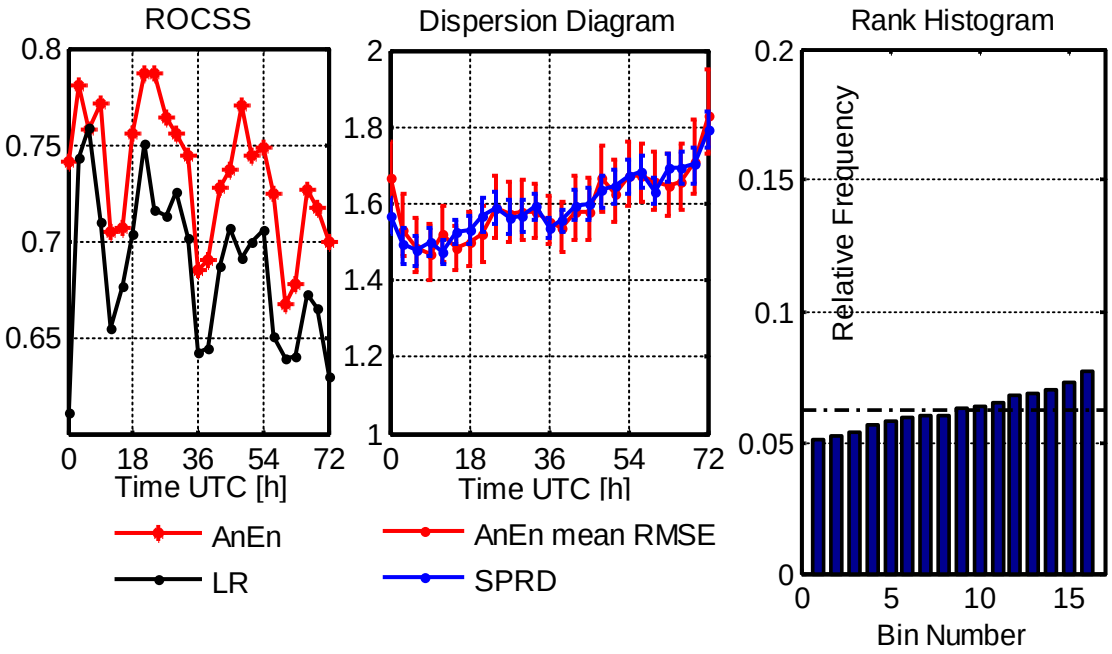

Figure 9. *Left: ROC skill score result for AnEn and LR forecasting depending on lead time. Middle: Dispersion diagram for AnEn forecasting. Right: Rank histogram for AnEn forecasting. All results refer to 14 locations in Croatia during year 2012.*

Figure 9 consists of ROC skill score results for AnEn and LR forecasting depending on lead time, dispersion diagram and rank histogram for AnEn forecasting. Results regarding ROC skill score show that the AnEn performs better than LR regarding forecast ability to discriminate between two possible outcomes (when wind speed did or did not exceed 5 ms^{-1}). Better result for AnEn forecasting system is probably due to LR's difficulty to fit a dependable regression line in case of the event is rarely observed within the training dataset, as it is the case here.

Statistical consistency is examined via dispersion diagram and rank histogram, only for AnEn forecasting. The LR forecasting is not included because in its standard formulation (the one

adopted in this study) it does not provide an actual ensemble, just a probability for a given event threshold. The rank histogram of AnEn indicates slight underestimation of wind speed among ensemble members. These results are consistent with the results presented in Delle Monache et al. (2013) and the time-lagged ensemble forecasting in Lu et al. (2007). To see how statistical consistency varies with lead time, a dispersion diagram can be plotted. Dispersion diagram shows that the mean square error of the ensemble mean matches the average ensemble variance, suggesting that AnEn is properly dispersive. The impact of the increase in horizontal resolution of starting model yielded mixed results (higher reliability, lower resolution).
Finally, different predictors were tested by comparing the root-mean-square error, rank correlation coefficient and bias of deterministic forecasting the mean of AnEn. Wind speed and direction, air temperature and buoyancy frequency seem to be the most important predictors.

Self-Organizing Maps-based ocean currents forecasting system

An ocean surface currents forecasting system has been developed for a coastal area of the northern Adriatic (Kalinić et al. 2016), based on a Self-Organizing Maps (SOM) neural network algorithm, high-frequency (HF) ocean radar measurements and numerical weather prediction (NWP) products (Vilibić et al. 2016b). The resulting currents were compared with operational ROMS-derived surface currents (Janeković et al. 2014). The two systems differ significantly in architecture and algorithms, being based on either unsupervised learning techniques or ocean physics. To compare performance of the two methods, their forecasting skills were tested on independent datasets (Vilibić et al. 2016a). The SOM-based forecasting system has a slightly better forecasting skill, especially during strong wind conditions, with potential for further improvement when data sets of higher quality and longer duration are used for training.

4.3.5 Ensemble Prediction System

4.3.5.1 In operation

The operational LAMEPS system is maintained by ZAMG-Austria and developed by RC-LACE.

4.3.5.2 Research performed in this field

Team members were involved in the development of the ALADIN_LAEF system in ZAMG.

4.3.5.3 Operationally available EPS Products

ECMWF EPS and ALADIN-LAEF products are available to forecasters.

Outputs of other operational ALADIN models run in other LACE countries together form an ensemble of forecasts since all meteorological services run different model versions and data assimilation/initialization set-ups.

4.4 Nowcasting and Very Short-range Forecasting Systems (0-6 hrs)

4.4.1 Nowcasting system

4.4.1.1 In operation

In the operational forecast service nowcasting is primarily based on METEOSAT satellite data, received through EUMETCast service, radar data from two Doppler radars located in the continental part (Bilogora and Osijek) and lightning data from LINET lightning detection network and ATD NOS system (Met Office).

Satellite data

- Meteosat Second Generation single channel data
- RGB images and image differences: all standard RGB images are available in 15 or 5 min (Rapid Scan Service) intervals, DAWBEE User Station used for processing and visualization of satellite data

Satellite-based Nowcast products

- Locally developed post-processing products based on satellite data
- EUMETSAT MPEF (Meteorological Products Extraction Facility) products received through EUMETCast service
- NWC SAF (Satellite Application Facility on support to Nowcasting/ and Very Short-Range Forecasting) products calculated by locally installed NWC SAF software using METEOSAT data ECMWF NWP and lightning data.

Products are received or calculated with each satellite scan (mostly in 15 min cycle) and displayed in the forecast intranet system.

INCA

The high-resolution analysis and nowcasting system developed at ZAMG, Austria has been implemented at DHMZ. INCA (Integrated Nowcasting through Comprehensive Analysis) combines forecast fields of the numerical weather prediction model ALADIN and high-resolution topographic data with measurements from surface station data and remote sensing data (radar, satellite). The system operates at a 1-km horizontal resolution and with vertical resolution of 100-200 m. In the current implementation at DHMZ, the INCA system provides analysis of 2-meter temperature, humidity and 10-meter wind on an hourly basis. Also two-dimensional maps of some derived quantities (e.g. CAPE, CIN, LFC, wind chill …) are available. Currently, the remote sensing data are not used as input for INCA. Also, the nowcasting part of INCA is not yet implemented.

4.4.1.2 Research performed in this field

4.4.2 Models for Very Short-range Forecasting Systems

4.4.2.1 In operation

4.4.2.2 Research performed in this field

4.5 Specialized numerical predictions

4.5.2 Specific models

4.5.2.1 In operational

4.5.2.2 Research performed in this field

4.5.2.2.1. Air quality modelling

EMEP model. New version of the EMEP rv4.3 (European Monitoring and Evaluation Programme) model has been released in 2013. It is installed and run at MHSC (Figure 10). Unified EMEP models are the chemical transport models used and developed at the Norwegian Meteorological Institute (Simpson et al, 2003). It simulates atmospheric transport and deposition of acidifying and eutrophying compounds, as well as photo-oxidants and particulate matter over Europe. The main

change is that daily meteorological input data used for the EMEP/MSC-W Model are based on forecast experiment runs with the Integrated Forecast System (IFS), a global operational forecasting model from the European Centre for Medium-Range Weather Forecasts (ECMWF). The IFS forecasts have been run by MSC-W as independent experiments on the HPCs at ECMWF with special requests on some output parameters. The meteorological fields are retrieved on a 0.2x0.2 rotated spherical grid and interpolated to 50x50 km2 polar-stereographic grid projection. Vertically, the fields on 60 eta levels from the IFS model are interpolated onto the 20 EMEP sigma levels.

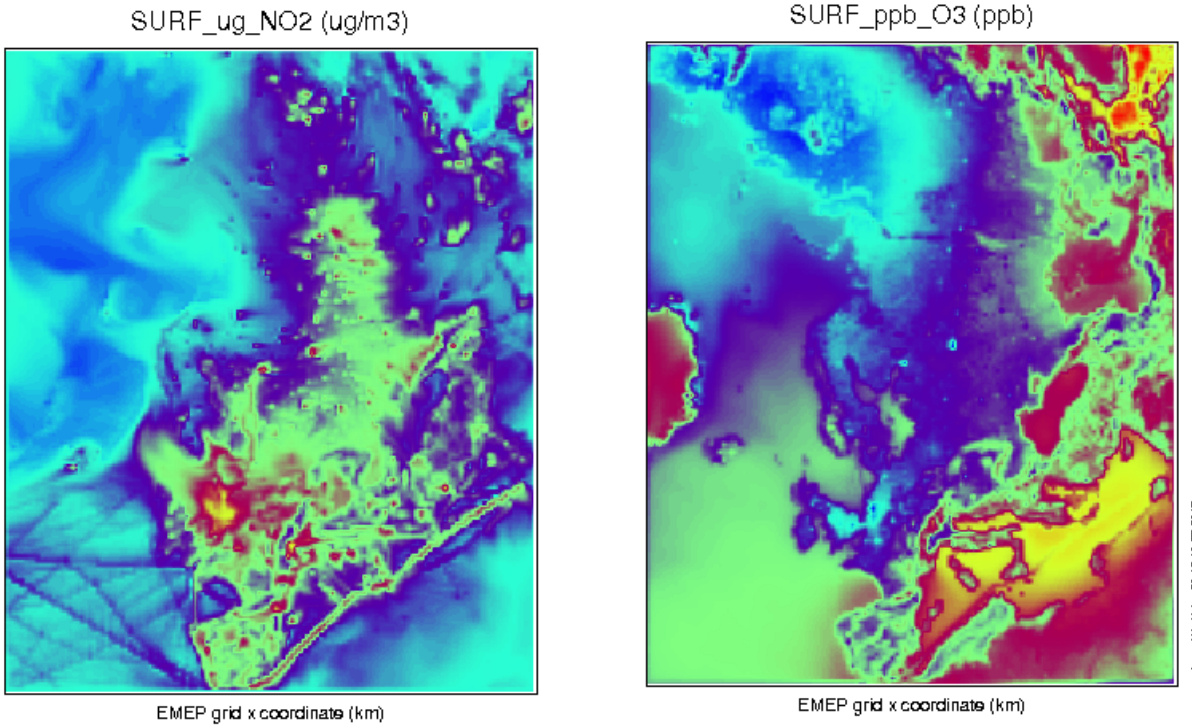

Figure 10. *Results of the EMEP rv3.4 model coupled with ESCWF for NO2 (left) and ozone (right).*

EMEP4HR Special application of the air quality model EMEP called EMEP4HR (EMEP for Croatia; e.g., Jeričević et al., 2007; 2009; 2010; 2011; Kraljević et al., 2008) has been developed at higher resolution, and coupled with NWP meteorological driver ALADIN at 10 km x 10 km horizontal resolution. Therefore the EMEP4HR model is EMEP Unified Eulerian model at finer resolution, 10 km x 10 km which uses ALADIN Numerical Weather Prediction (NWP) model. The model is used for the modelling of atmospheric chemistry and calculation of photo-oxidants and particulate matter concentrations over domain shown in Figure 11. The EMEP4HR model is nested into the unified EMEP model that is operationally applied on horizontal resolution 50 km x 50 km.

Spatial distribution of yearly average surface concentrations for NO_2, O_3, PM_{10} and NH_3 over the EMEP4HR domain is shown in Figure 12 (Setup with PARLAM model). The model results have been used in different research studies to analyze the simulation of air pollutants in complex urban orography over city of Rijeka in Croatia (Telišman et al. 2009; 2012).

The model was used in the modelling intercomparison study AQMEII (Air Quality Model International Initiative) and the results are published in Vautard et al. (2011) and Solazzo et al. (2012).

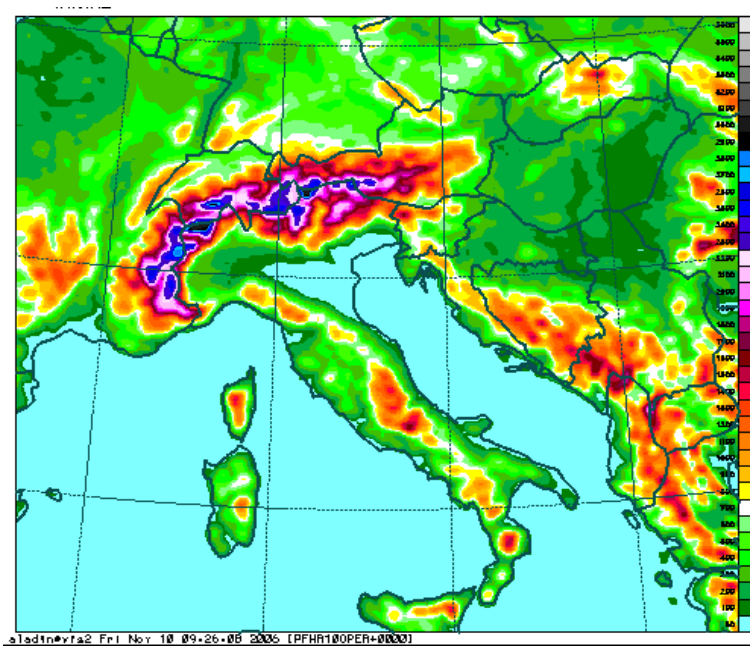

Figure 11. *Domain of the EMEP4HR model (EMEP coupled with NWP ALADIN) with 10km x 10km horizontal resolution.*

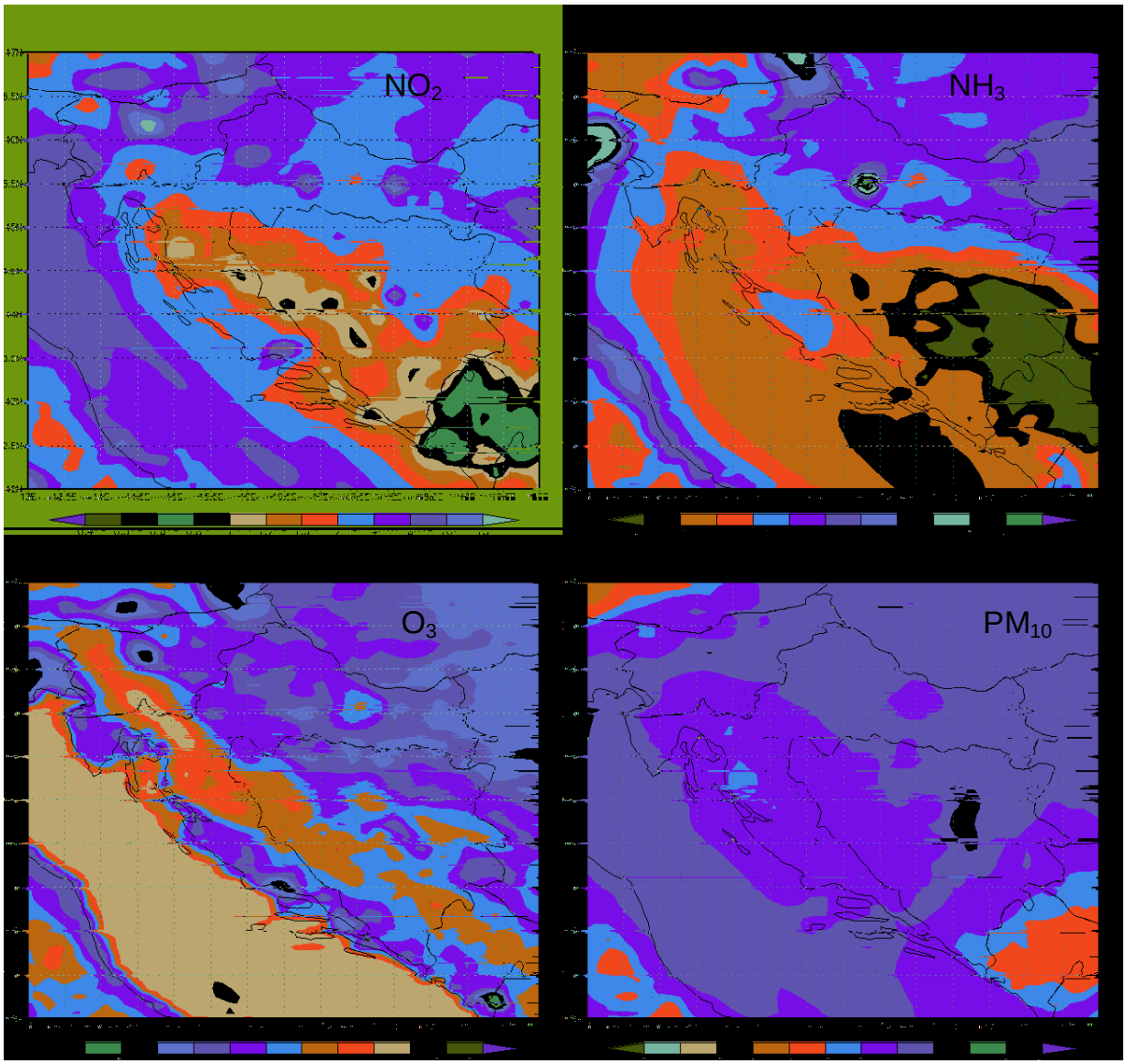

Figure 12. *Spatial distribution of yearly average surface concentrations for different pollutants in the EMEP4HR domain.*

WRF MODEL is used for air quality modelling research due to many advantages since many models are developed to be coupled with WRF and its basic characteristics such as good performance and good operational application. Numerical weather prediction (NWP) simulations are preformed (Figure 13 and Figure 14) with mesoscale version of Weather Research and Forecasting (WRF – ARW 3.1.1) model. The WRF simulation for this case study is run using a Lambert conformal projection and two-way nested grids with horizontal resolution of 9-km, 3-km and 1-km, respectively. The vertical grid has 28 terrain-following hydrostatic pressure coordinate levels with the top level located at 50 hPa. Initial and boundary conditions were updated every six hours with data from Global Forecast System (GFS) at a 1° resolution. The physical schemes used in this study are: WSM 3-class simple ice scheme for microphysics (Hong et al., 2004), a Rapid Radiative Transfer Model – RRTM (Mlawer et al., 1997) for long wave radiation, MM5 Shortwave scheme (Dudhia, 1989) for short wave radiation, Monin-Obukhov scheme (Monin and Obukhov, 1954) for surface layer options, and Yonsei University (YSU) planetary boundary layer (PBL) scheme (Hong and Dudhia 2003), which is a modification of the Medium-Range Forecast (MRF) scheme based on Troen and Mahrt (1986) to include explicit entrainment fluxes of heat, moisture and momentum, counter-gradient transport of momentum, and different specification of the PBL height.

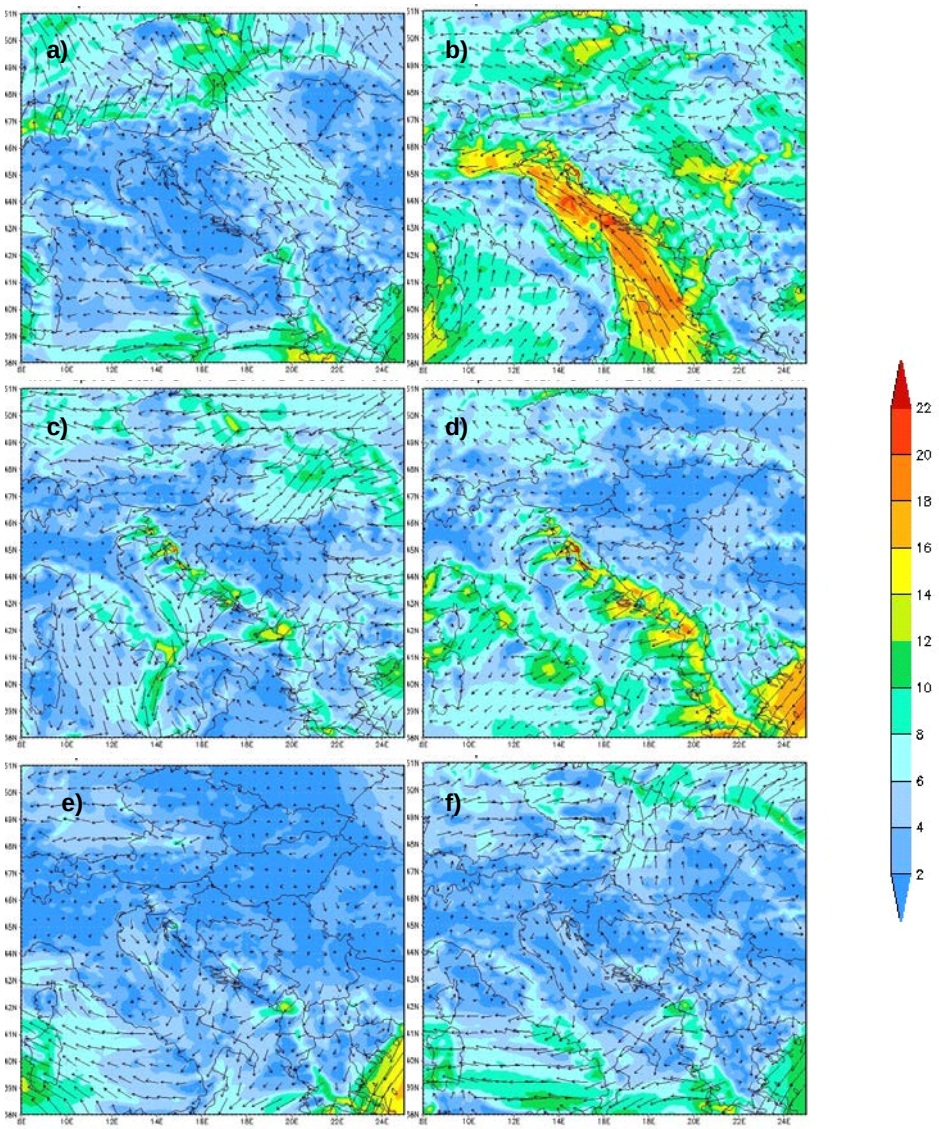

***Figure 13**. The spatial distribution of surface wind speed and direction calculated with WRF model at 18 UTC for: a) 2 November, b) 6 November, c) 10 November, d) 12 November, e) 15 November and f) 17 November in 2011.*

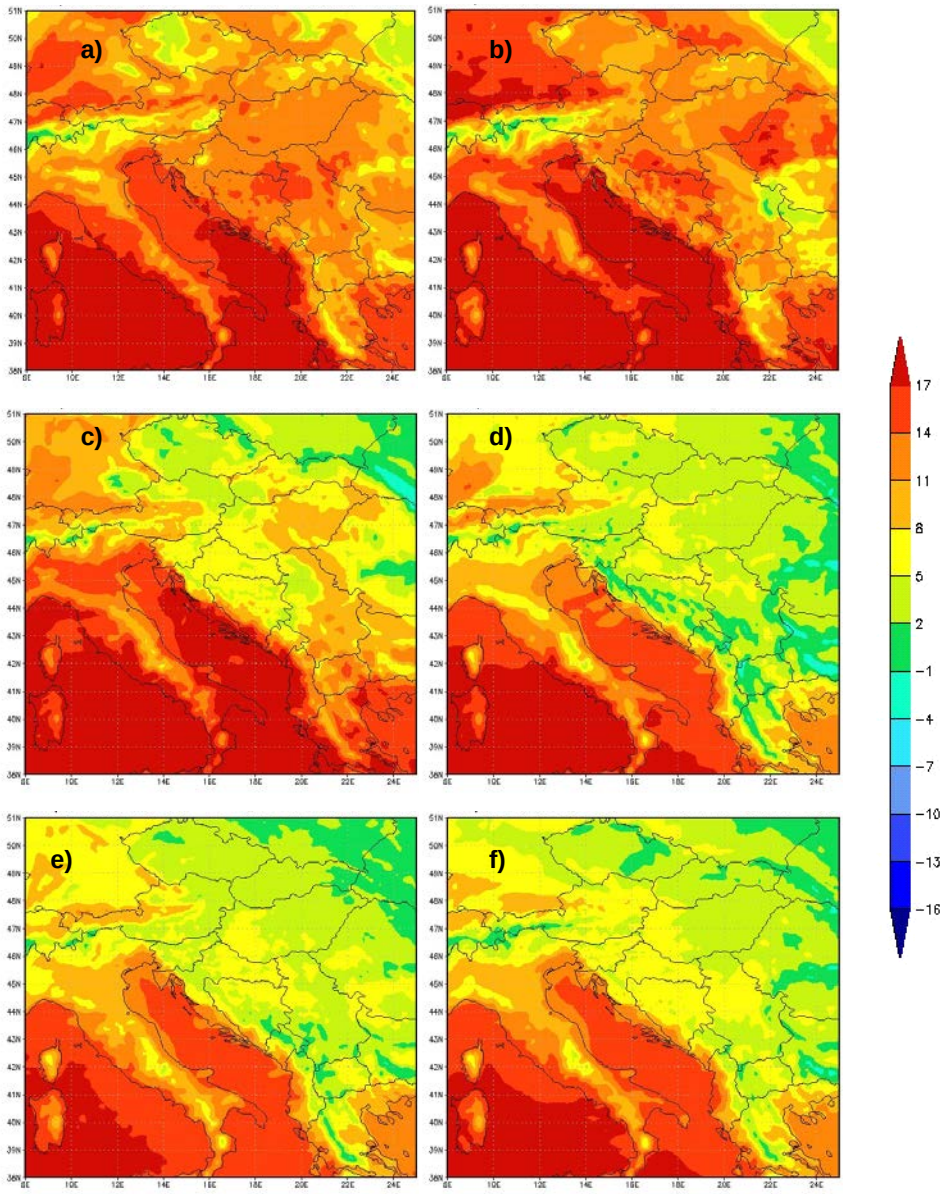

Figure 14. *The spatial distribution of 2 m air temperature (° C) calculated with WRF model at 12 UTC for: a) 2 November, b) 6 November, c) 10 November, d) 12 November, e) 15 November and f) 17 November in 2011.*

Hysplit model. The Hybrid Single-Particle Lagrangian Integrated Trajectory (HYSPLIT) developed at the National Oceanic and Atmospheric Administration Air Resources Laboratory (NOAA ARL) is a system for computing atmospheric trajectories, complex dispersion and simulations using either puff or Lagrangian particles (Draxler 1997, 2007). The backward HYSPLIT trajectories were calculated by running the model without dispersion, thus computing the advection of a single pollutant particle within the mean wind. The gridded meteorological data fields required to run HYSPLIT were obtained from archived data sources at NCEP i.e., global latitude/longitude data from the Global Forecast System (GFS) model at 1° horizontal resolution. It has been applied in research as well as in accidental situations (Figure 15).

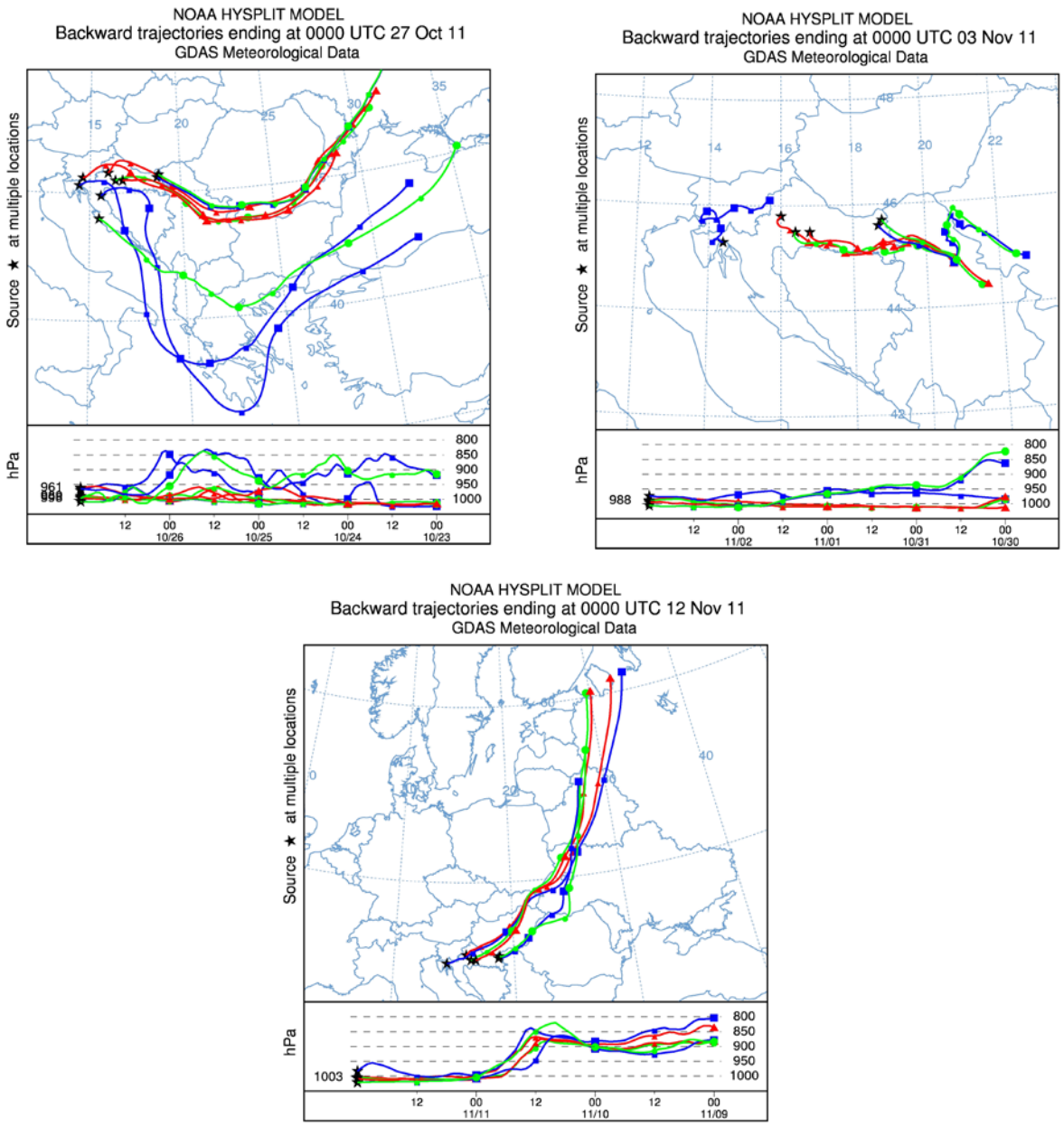

Figure 15. *Four days backward trajectories arriving to sites in Croatia (colours are randomly chosen for different locations) at 00 UTC on: a) 27 October, b) 3 November during the first episode and c) 12 November 2011.*

4.5.2.2.2. Regional climate modelling

DHMZ supports several regional climate modelling activities. The main modelling tool is hydrostatic regional climate model RegCM4 (Giorgi et al. 2012). Additionally, results of the EU FP6 project ENSEMBLES (van der Linden and Mitchell 2009) and EURO-CORDEX (e.g., Vautard et al. 2013) activities are used in estimating the uncertainty related to model formulation. Standard analysis includes an evaluation of the model systematic errors and estimation of historical and projected climate changes and trends. Results are published in scientific papers as well as in the national reports on climate change (MZOIP 2014). The regional climate modelling group is active in introducing obtained results to various stakeholders in the process of mitigation and adaptation on climate change.

In the rest of this subsection, we will present results of the evaluation of the EURO-CORDEX regional climate models' (RCM) simulations over Croatia and neighouring countries.

Models evaluated

Three groups of models are evaluated in this report:

(1) an ensemble of ERA-Interim driven RCMs from the EURO-CORDEX initiative. These RCMs cover European domain with the minimum of the CORDEX specified domain size. Period 1989-2008 from all RCMs in this ensemble is evaluated.

(2) an ensemble of RCMs from the EURO-CORDEX initiative driven by the CMIP5 GCMs. RCMs in this group cover same domain and have the same model setup as their ERAInterim-driven partners in group (1). The only relevant differences are (a) the use of CMIP5 GCMs as the source of lateral and SST (for some models also sea-ice) boundary conditions, and (b) the coverage of different period. The consequence of the boundary conditions from the coupled GCM is the independence from the observed temporal variability. Nevertheless, the model period 1971-2000 (with the same historical greenhouse-gases concentrations) is used to estimate RCM performance versus observations for the same period.

(3) DHMZ set of EURO-CORDEX simulations forced by ERAInterim and GCMs. At the time of this report, only 0.44°/50km and 0.11°/12.5km simulations of RegCM4 (Giorgi et al. 2012) model forced by the ERA-Interim reanalysis were available from the ESGF database. These two simulations are referred to as DHMZ-ERA-44 and DHMZ-ERA-11. In the GCMs-driven set of DHMZ RegCM4 simulations additionally performed, four CMIP5 GCMs are downscaled to 50 km resolution (HadGEM2-ES, MPI-ESM-MR, EC-EARTH and CNRM-CM5) and two CMIP5 GCMs (MPI-ESM-MR and EC-EARTH) are downscaled to 12.5 km resolution. Some major errors in reproducing precipitation climatology are found in DHMZ RegCM4 12.5km simulation (i.e., DHMZ-ERA-11). In order to address this issue, additional 12.5 km ERAInterim-driven simulation is performed, where only convection scheme in RegCM4 is replaced from the MIT scheme to Grell scheme. This final simulation is referred to as DHMZ-ERA-11-GRELL.

Observations

To evaluate near-surface (i.e., 2 meter) air temperature T2m and total precipitation amount R in previously defined sets of RCM simulations, we use pan-European gridded dataset E-OBS (version 11) at the regular 0.25° grid. The quality of E-OBS dataset is thoroughly evaluated in many studies, so limitations concerning e.g., the precipitation undercatch, underlying station density and interpolation method are known. In this report, it will be used to estimate RCMs' performance over land, and for the two periods (1989-2008 for the ERAInterim-driven set of simulations; 1971-2000 for the GCMs-driven set of simulations).

Evaluation

Regions of interest

The focus of this study is region centered over Croatia (CRO region in the rest of this paper; it covers 13°E-20°E, 42°N-47°N), which also includes the whole Slovenia and Bosnia and Herzegovina, and parts of neighbouring countries. This region includes complex coastline and many islands along the eastern Adriatic, mountain chains over most of the region, and parts of the Pannonian basin in the northern and north-eastern parts.

Interpolation methods

Before computing specific measures/score, different models and E-OBS observation are set to the common grids in the following manner:

(1) 0.11°/12.5 km RCMs' fields of daily T2m and R (and static topography height field) are spatially averaged 2×2 grid-cells (resulting in 0.22°/25km grids specific to each RCM), and bilinearly interpolated to the regular 0.25°×0.25° E-OBSv11 grid (now common grid to all high-resolution RCMs).

(2) 0.44°/50 km RCMs' fields of the same quantities are bilinearly interpolated to common 0.5°×0.5° grid. This common 0.5°×0.5° grid is based on EOBSv11 spatially averaged over 2×2 grid cells from the default 0.25°×0.25° grid, and these upscaled EOBSv11 fields are used to evaluate low-resolution RCMs.

(3) ERA-Interim and CMIP5 GCMs are bilinearly interpolated from their specific grids to common 0.5°×0.5° grid, and evaluated against the upscaled EOBSv11 fields.

For T2m, interpolated fields are adjusted to height difference between interpolated topography height and E-OBS topography, using free-atmosphere lapse rate of -0.65 °C/100 m. Since we are dealing with analysis over large areas and mean multi-year monthly and seasonal time-scales, the assumption of constant lapse rate is justifiable. In short, 0.11°/12.5km RCMs are upscaled to common 0.25°×0.25° grid and evaluated against original EOBSv11 observations, while 0.44°/50km RCMs and GCMs are only interpolated to the common 0.5°×0.5° grid.

Results

For the purpose of this report, we shall limit to evaluation of winter (i.e. DJF) spatial variability of the precipitation and 2m air temperature fields, and systematic errors through all four climatological seasons (winter/DJF, spring/MAM, summer/JJA, autumn/SON). The color- and mark- coding of all models are summarized in Figure 16**.**

Figure 16. *Color- and mark- coding of models evaluated in this report. Different color represents different boundary conditions (ERAInterim or CMIP5 GCMs) while different mark type represent different regional climate model.*

Seasonal biases

Precipitation

Mean seasonal precipitation bias spatially averaged over CRO is summarized in Figure 17 Almost all RCMs have wet bias during winter. In simulations forced by ERA-Interim reanalysis wet bias is generally well below 50%. Outliers include CNRM-ERA with almost zero winter bias and DHMZ-ERA with strong overestimation of winter precipitation in 0.11° simulations. In DHMZ-ERA-11 simulation winter precipitation is more than doubled when compared to E-OBSv11. In simulations forced by the GCMs, the range of errors is increased and now DHMZ-ECEARTH-11 and DHMZ-MPI-ESM-MR-11 stand out as outliers. For RCMs where 0.11°-0.44° partners are available, an increase in the precipitation amount in 0.11° simulations is found when compared to 0.44° partners.

Mixture of different amplitude and sign of the biases is present for the summer season (Figure 17). Almost all 0.44° and ERA-Interim simulations have dry bias (with IPSL-ERA-44 close to zero) while typical precipitation amount increase in the 0.11° simulations changes the sign of the precipitation bias in 3 out of 7 RCMs (IPSL-ERA, DHMZ-ERA and CNMR-ERA). DHMZ-ERA simulations are comparable in terms of the summer precipitation errors to the rest of the ERA-Interim forced simulations at both resolutions. This implies the DHMZ model setup with the MIT convective scheme is well designed for the summer season when 0.11°/12.5km resolution is applied. In the group of the GCM-driven simulations larger spread of the model errors is found. In most cases the increase in the spatial resolution resulted with an increase in the precipitation amounts; this improves dry bias in most 0.44° simulations, but increases already wet bias in 0.44° simulations for CLM-ESM and CNRM-Cm5 simulations. Two models don't follow this general rule: in IPSL-CM5A and SMHI-Cm5 wet bias present in 0.44° simulations is slightly reduced in 0.11° simulations.

DHMZ-ERA-11-GRELL simulation performs better in general over the CRO region. The relative systematic errors in total precipitation amount are reduced from ~100% to ~75% during DJF, from ~100% to ~50% during MAM and from ~50% to ~10% during SON. During summer (i.e., JJA), DHMZ-ERA-11-GRELL changed the sign and increased the magnitude of the bias when compared to DHMZ-ERA-11, but is still comparable to the rest of the ensemble (especially, several 0.44° simulations). In summary, the change of the convective scheme is beneficial for DHMZ-ERA-11 simulations in terms of the mean precipitation biases.

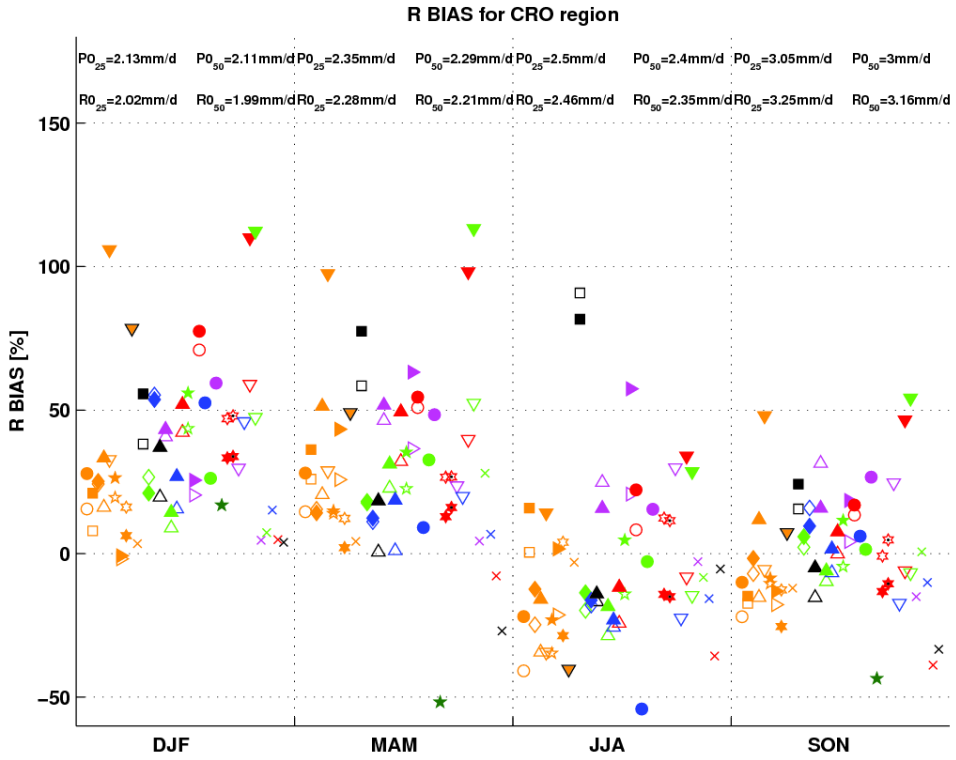

Figure 17 *Mean seasonal (winter/DJF, spring/MAM, summer/JJA, autumn/SON) total precipitation R bias averaged over CRO region (land-only) for ERA-Interim-driven and GCM-driven 0.11°/12.5 km and 0.44°/50 km RCMs and their corresponding driving global models. All GCMs and ERA-Interim are first bi-linearly interpolated to common 0.5°×0.5° grid. All units in %.*

Near-surface air temperature

EURO-CORDEX temperature errors averaged over CRO region are summarized in Figure 18 Starting from winter, all ERA-Interim forced simulations show good performance, with mean errors of models at both resolutions from almost -3 °C (KNMI-ERA-11) to 1 °C (IPSL-ERA-44). DHMZ-ERA performs well with absolute errors at two resolution well below 1 °C. As expected, the spread of the GCM-driven simulations is larger than the spread of the ERA-Interim driven RCMs, with e.g. three SMHI 0.44° simulation having warm biases between 1 °C and 2 °C. In DHMZ-ECEARTH there is positive impact of the increased spatial resolution with cold bias in 0.11° run less than 0.5 °C. At the same time, the impact of the resolution is minor for some models (e.g. winter season for the IPSL-ERA, IPSL-CM5A and CLM-ESM). Also, the impact of the alternative convective scheme in DHMZ-ERA 12.5km simulations is generally positive over all four regions during winter.

Concerning the DHMZ-ERA, simulated 2m temperature errors are generally inside the range of other EURO-CORDEX simulations. The warm bias in 0.44° simulation present over all four regions during summer is substantially reduced in the 0.11° simulation. Over CRO region warm bias in the 0.44° DHMZ-ERA simulation is substantially reduced in the 0.11° during summer. DHMZ-ERA-11-GRELL shows small reduction of the mean biases in DJF, MAM and SON. For this experiment, similar to precipitation, temperature errors in JJA are increased (we have combination of the dry and warm bias) but are close to the rest of the ensemble.

The impact of the resolution increase has mixed effects for different models. However, over CRO region, KNMI and SMHI models forced by ERA-Interim simulate lower temperatures in 0.11° simulations compared to 0.44° partners in all seasons. This is also confirmed in almost all GCM-driven runs of these two models.

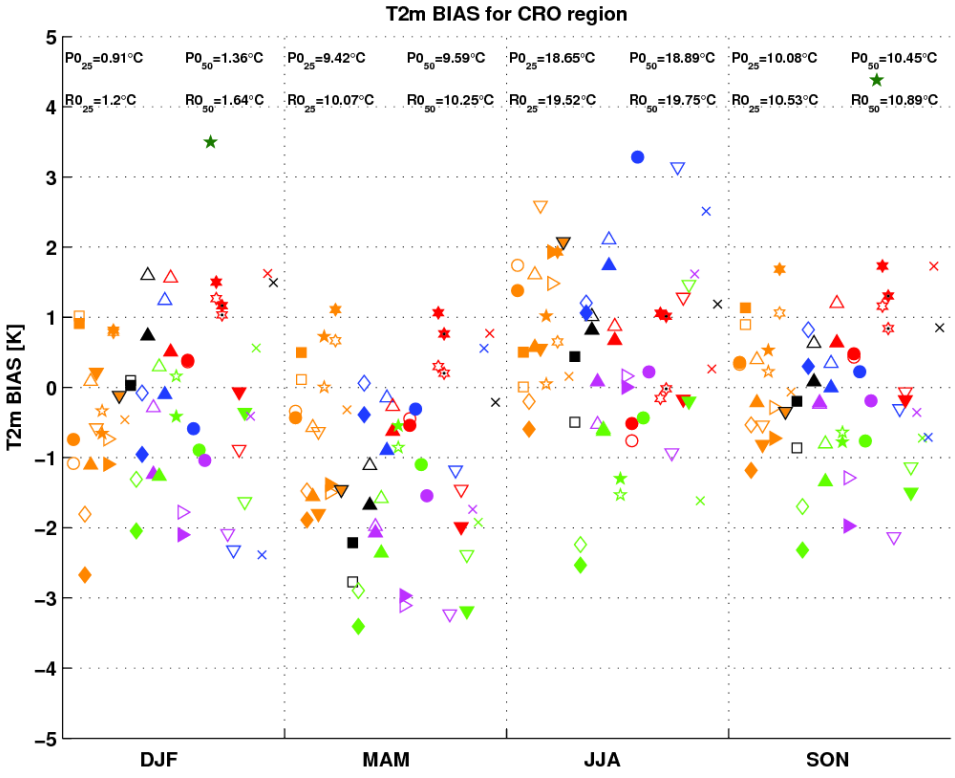

Figure 18 *Mean seasonal (winter/DJF, spring/MAM, summer/JJA, autumn/SON) T2m errors averaged over CRO region (land-only) for ERA-Interim-driven and GCM-driven 0.11°/12.5 km and 0.44°/50 km RCMs and their corresponding driving global models. All GCMs and ERA-Interim are first bi-linearly interpolated to common 0.5°×0.5° grid. All units in °C.*

Spatial variability

Precipitation

Mean winter precipitation is well correlated in space with E-OBSv11 in both ERA-Interim forced and GCM-driven simulations, with spatial correlation coefficient PACO from 0.5 to more than 0.8 (Figure 19). The spatial variability in terms of the normalized standard deviation RSV is reproduced excellent by two 0.44° simulations: CLM-ERA-44 and CNMR-ERA-44. There is tendency of 0.11° simulations to increase the spatial variability of the mean winter precipitation when compared to their 0.44° partners and E-OBSv11 observations. Also, in most cases the higher-resolution PACO between RCMs and E-OBSv11 is slightly increased. Although DHMZ-ERA-11, DHMZ-ECEARTH-11 and DHMZ-MPI-ESM-MR-11 are three out of four models with highest RSV, they are correlated well with E-OBS, attaining PACO between 0.6 and 0.7. Also, DHMZ-ERA-11-GRELL only slightly reduces the PACO and RSV when compared to the default DHMZ-ERA-11 simulation.

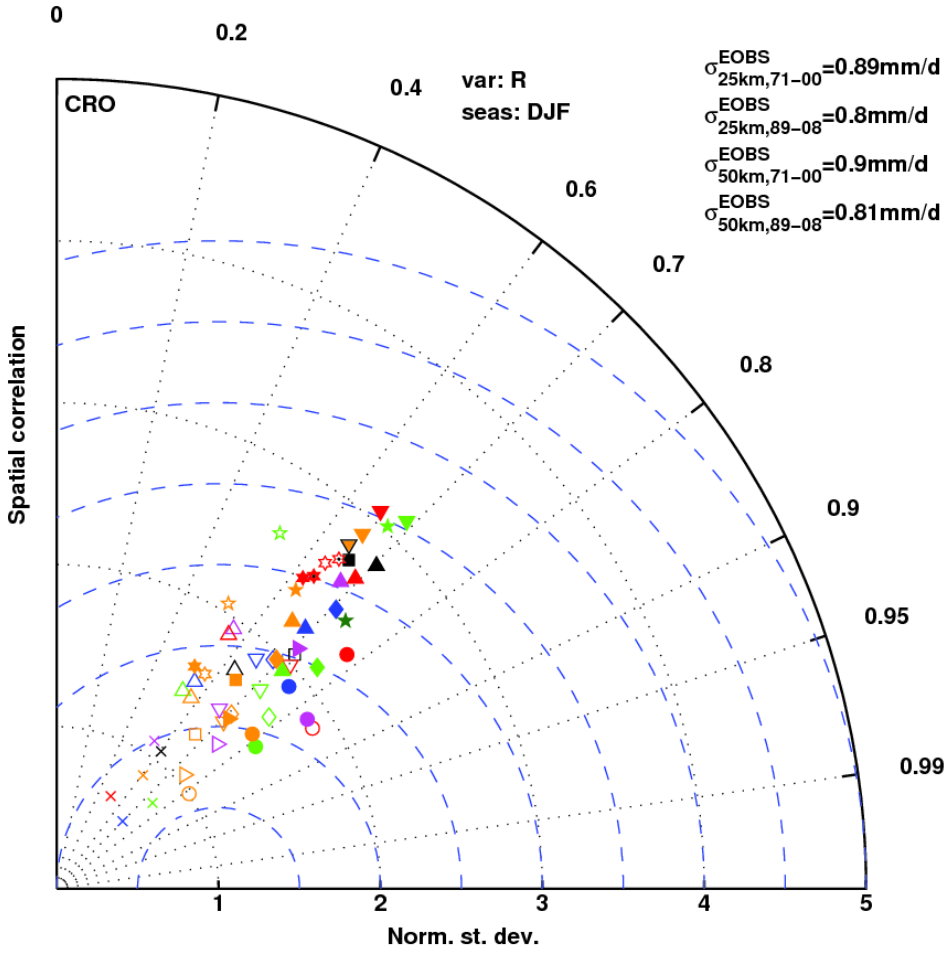

Figure 19 *Taylor diagram of mean winter total precipitation amount R in ERA-Interim and GCM-driven ensembles. RSV (the radius) is the ratio of spatial standard deviations over CRO region in RCMs (and GCMs) over E-OBSv11, and PACO (the angle) is spatial correlation coefficient over CRO region between RCMs (and GCMs) and E-OBSv11. Blue-dashed lines are centered root-mean-square differences between models and E-OBSv11 in space. In the panel left corner are relevant spatial standard deviations of the E-OBSv11 over two grids (0.25°×0.25° and 0.5°×0.5°) and for the fields averaged over the two periods (1989-2008 and 1971-2000) in mm/d.*

Near-surface air temperature

The variability of the mean winter and summer 2m temperature over the region CRO is summarized in **Figure 20**.

In terms of spatial variability, there is excellent performance of all models with spatial correlation coefficient PACO against E-OBSv11 generally more than 0.8 in winter (**Figure 20**), while normalized standard deviation RSV ranges from approximately 1.0 to less than 1.5. For this region and scores, the DHMZ simulations are by no means outliers and fit well to the rest of the ensemble. Additionally, DHMZ-ERA-11-GRELL is comparable to (already well performing) DHMZ-ERA-11 with some minor impacts on both mean winter and summer temperature PACO and RSV over CRO region.

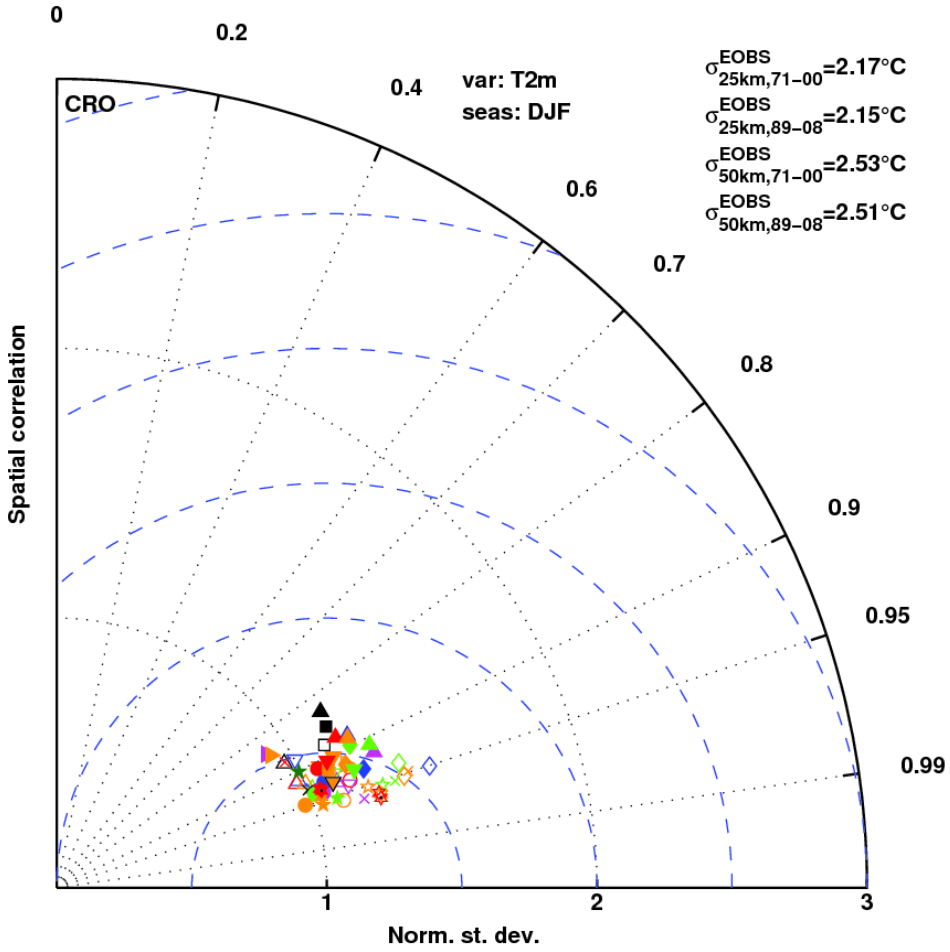

Figure 20 *Same as Figure 19 but for the mean winter (DJF) near-surface temperature T2m over CRO.*

4.5.3 Specific products operationally available

Forecast of the road conditions. The variability of bora wind (bura) in space and time has a pronounced influence on road traffic. Therefore, knowing Bura characteristics is a necessary condition for road transport safety. To properly organize the traffic safety system, special emphasis should be given to the quality of measured long term wind speed and direction data and low resolution atmospheric forecast models.

An application, named ANEMO-ALARM (Bajić et. al., 2008), has been developed that assists road authorities in managing the traffic on the roads affected by strong wind and turbulence. The application is based on measured and forecasted wind speed and gusts for a choice of locations on Croatian roads that are most affected by severe wind. The application communicates with the user through a graphical user interface (Figure 21). The interface shows current and expected alarm status for road traffic safety conditions for any of the three categories of vehicles (green is for open road, yellow for preparedness status and expected road closure and red indicated that the road is closed).

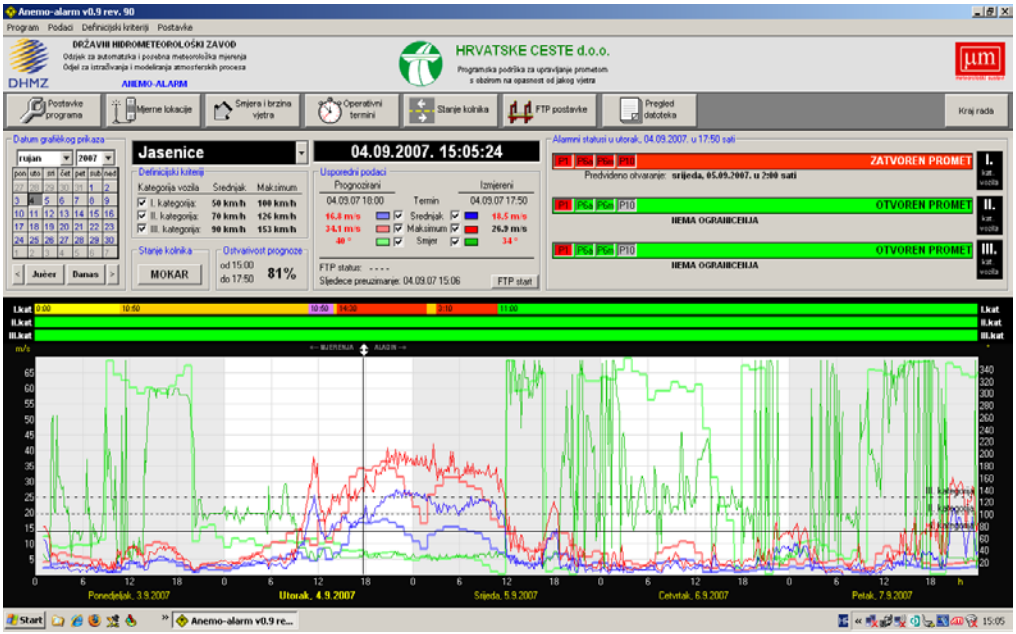

Figure 21 *The ANEMO-ALARM user interface. The measured (thick lines) and modelled (thin line) mean wind speed is shown on a graph as blue line, wind gusts are red and direction is green.*

4.6 Extended range forecasts (ERF) *(10 days to 30 days)*

4.6.1 Models

4.6.1.1 In operation

Locally none (ECMWF products are used).

4.6.2 Operationally available NWP model and EPS ERF products

DHMZ participates at SEECOF (South-Eastern Europe Climate Outlook Forum) which is currently leaded by SEE Sub-regional Virtual Climate Change Centre (SEE-VCCC). Seasonal forecasts for winter (December, January, February) and summer (June, July, August) are performed by

consensus of NMHS representatives and end users and qualitative verification of such forecasts is made.

4.7 Long range forecasts (LRF) *(30 days up to two years)*

4.7.1 In operation

Locally none (ECMWF products are used).

4.7.2 Research performed in this field

Locally none (ECMWF products are used).

4.7.3 Operationally available EPS LRF products

5. Verification of prognostic products

5.1 In operation

In the Forecast office, the emphasis of the verification is recently put to the office's end products (special forecasts, warnings etc.). Figure 22 presents an example of operational (daily and monthly) real-time verification, where a comparison of maximum and minimum temperature forecasts is displayed, and basic scores are calculated.

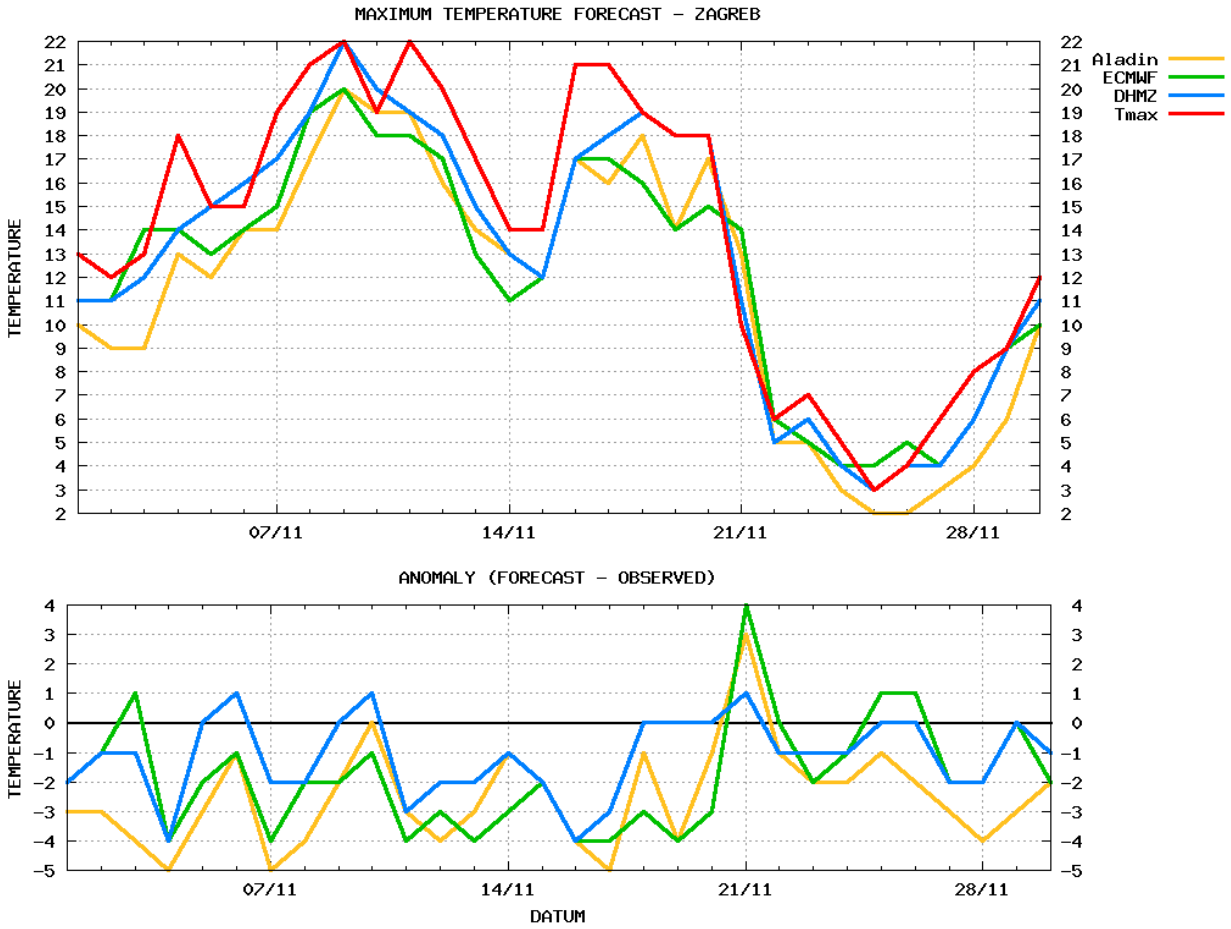

Figure 22 Real-time verification of 2m maximum temperature forecast (for tomorrow) for Zagreb Maksimir. for November 2015. Model forecasts (Aladin, ECMWF) are compared to Office's forecast (DHMZ) and observed values (Tmax). Basic scores are calculated: mean error (ME), mean absolute error (MAE) and root mean square error (RMSE). Skill is defined as percentage of forecasts where absolute error is less than 2°C.

For the model verification, some ECMWF verification is carried out on a yearly basis, and results are published in Annual Report on application and verification of ECMWF products ("Green book").

In the Research department, standard statistical scores: RMSE, STD and bias are computed using all conventional measurements available for the data assimilation: SYNOP, TEMP, SHIP and automatic stations (Tudor et al. 2015b). Also graphs with measured and modeled meteorological quantities are produced. Operationally, Research department produces graphs of measured meteorological quantities (mean sea level pressure, 2-m temperature and humidity, 10-m wind speed, direction and gusts) precipitation and observed cloudiness together with forecasts of the same parameter obtained from various operational model forecast runs from the closes model grid point. The same is done for SYNOP and automatic stations.

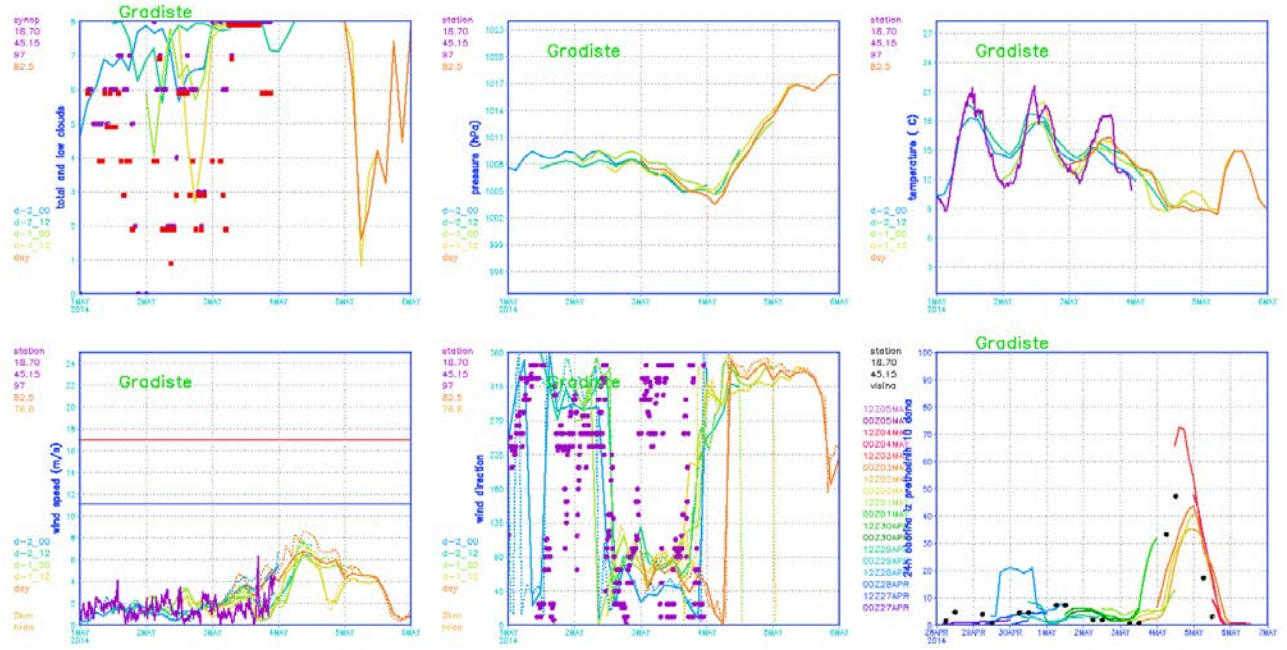

Figure 23. *Measured (purple, red or black marks) and forecast from 8km (full line) and 2km (dashed) wind forecast for cloudiness, mean sea level pressure, temperature (first row) and wind speed, direction and precipitation (second row). This is an example for a SYNOP station Gradište. Details are in the text.*

An example in Fig. 23 shows the comparison of measured and forecast data for the Gradiste SYNOP station, the longitude and latitude and station height are shown in the top left corner of each panel. First graph in Fig. 23 shows observed total cloudiness (purple marks) and low cloudiness (red marks), while other graphs at Fig. 23 (except last one) show measured mean sea level pressure, temperature, wind speed and direction during the previous two days and today, as well as forecasts during the same period and the next two days. The most recent forecast run (starting today at 00) is shown in orange, yesterday's run from 12 UTC analysis is in yellow, from 00 UTC is in light green, a day before yesterday at 12 UTC is in light blue and at 00 UTC is in blue. The accumulated 24-hourly precipitation is shown in Fig. 23 (last graph) for the previous 9 days, different line colors correspond to forecasts starting from different analysis times. The time of the analysis is written on the left side in the same color. The measured precipitation is shown with black dots. Similar graphs are produced automatically, every hour, after the measurements from SYNOP stations become available, for all Croatian SYNOP stations and a considerable number of SYNOP stations from the surrounding countries.

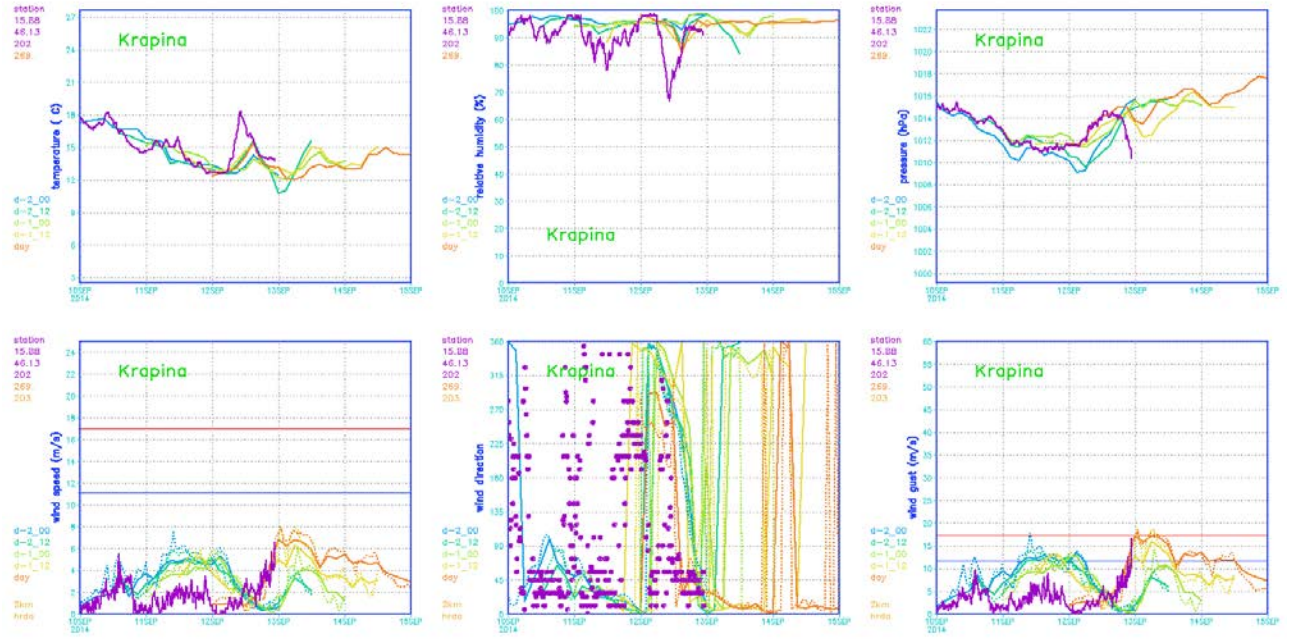

Figure 24. *Measured (purple) and forecast from 8km (full line) and 2km (dashed) wind forecast for temperature, relative humidity, mean sea level pressure (first row) and wind speed, direction and gusts (second row). This is an example for an automatic station Krapina. Details are in the text.*

There are more than 40 automatic stations that measure meteorological parameters in 10 minute intervals, these data are also used for operational model verification (Figure 24). This example shows the comparison of measured and forecast data for the automatic station Krapina, the longitude, latitude and height of the station are shown in the upper left corner. The comparison is made for temperature, relative humidity, mean sea level pressure, wind speed, direction and gusts. Measured values are plotted with 10 minute interval. The figures are made once per hour.

Objective scores, such as BIAS, RMSE, MAE, STD are calculated against SYNOP and Croatian automatic stations and TEMP observations covering ALADIN-Croatia domain. Temporal resolution is 6 hour for upper air verification against TEMP, 3 hour for screen level verification against SYNOP on ALADIN-Croatia domain and 1 hour for the verification against only Croatian meteorological stations. One example of such plots is shown at Fig. 25.

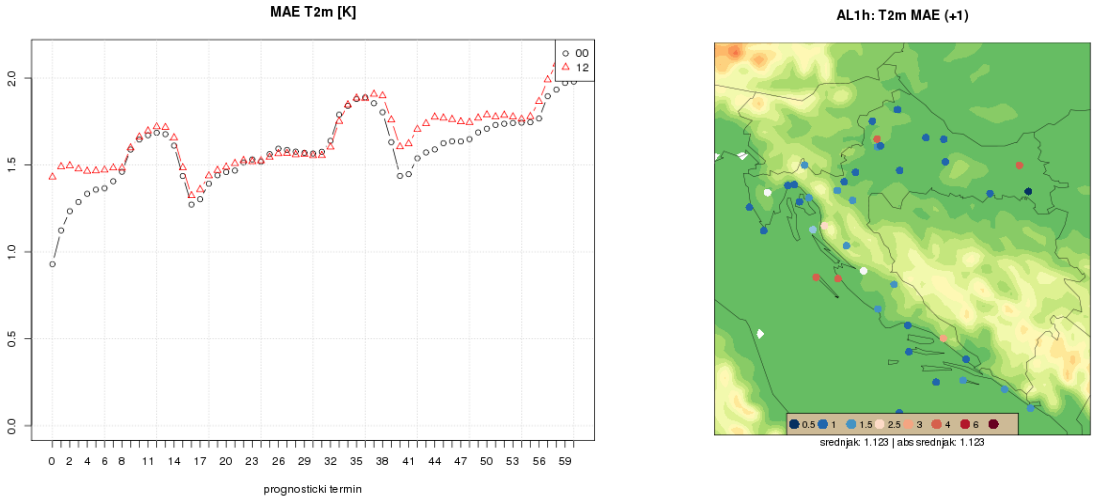

Figure 25. *Left: MAE of two ALADIN-Croatia runs initialized at 00 and 12 UTC against prognostic hour. Right: MAE for first prognostic hour at Croatian meteorological stations. Scores are calculated for July 2012.*

Additionally, number of scores based on contingency tables is calculated such as frequency bias, hit rate, false alarm ratio, false alarm rate, threat score, the equitable threat score…

Except local tools a verification tool developed in ALADIN community, called VERAL (verification for ALADIN, http://www.rclace.eu/File/NWP_Utility_Inventory/ ALADIN/Czech Republic/quest_CHMI_veral.doc) is installed at DHMZ and is used for operational verification as well as testing of new versions of model code available for operational forecast and various options and tunings before a new model version is introduced to the operational forecast suite. The VERAL program package produces standard deviation, bias and root mean square error of surface variables, such as 2m temperature and relative humidity, mean sea level pressure, wind components as well as wind speed and direction. It also computes the same statistical parameters in vertical-time cross sections for temperature, geopotential height, wind speed and direction and relative humidity on standard isobaric surfaces using vertical soundings available over the model domain.

Additionaly, HARMONIE verification package (Yang, 2008) has been ported locally. The operational forecast data are also sent to the joint centre for verification using the same package, so this also enables inter-comparison of model forecasts from different services (and hence different models, model versions, options, resolutions etc.). This verification package is more advanced and computes more scores when compared to VERAL and offers more flexibility.

Verification is performed using standard GTS data available via global exchange and high - resolution in - situ data from the national network (when possible). The measurements used for verification by the common tools such as the HARMONIE package mentioned previously are obtained from ECMWF, where the measured data are quality checked, flagged and discarded by an automatic procedure. Unfortunately, this means that some measured data during particular weather phenomena are discarded as wrong.

The performance of the operational forecast can be monitored on the intranet

http://noa.gric.dhz.hr/~aladinhr/veral-oper-00-06-12-18/HTML-DIR/ where the recent and historic products of the VERAL verification package can be accessed. The scores are computed monthly, seasonally and separately for cold/warm part of the year. The scores are computed for both surface and upper air fields, regularly after the period of interest finishes. The verification products for the operational forecast computed using HARMONIE verification package are also available via intranet on the page http://noa.gric.dhz.hr/~aladinhr/HARMONIEverif/ where a practical user interface allows a choice in the variable and score to be displayed, section 4.2 shows several examples of scores.

Subjective verification of precipitation: Subjective verification of precipitation is based on comparison of figures of 24h accumulated precipitation fields over ALADIN-Croatia domain from model (2km and 8km) with precipitation figures of measured precipitation. One example of such subjective verification is shown on Fig. 26.

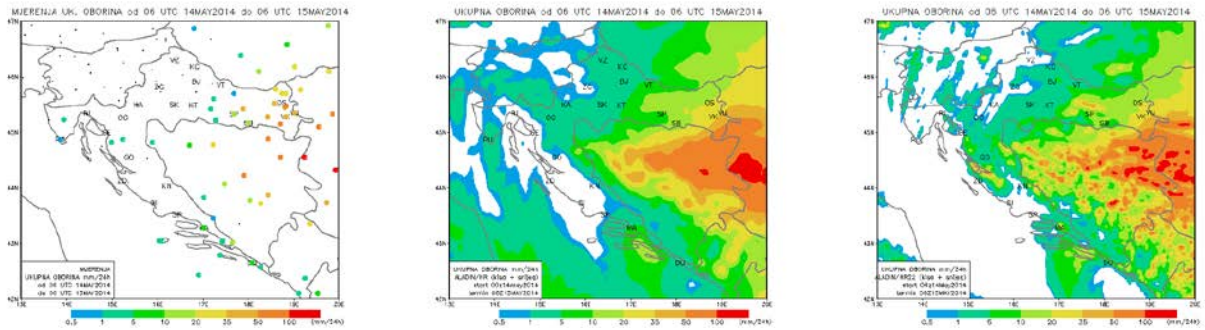

Figure 26. *24h accumulated precipitation from measurements from rain gauges (circles) (left), 8 km forecast (middle) and 2 km forecast (left) for 20140514 06 UTC – 20140515 06 UTC.*

5.2 Research performed in this field

Ongoing work on wind speed and direction verification including RMSE decomposition and quantitative spectral verification (Horvath et al., 2012) was extended to more stations from different climate regions of Croatia. Verification of operational 10 m wind forecast obtained from ALADIN mesoscale numerical weather prediction model was performed for ALARO 8 km (AL8) and simplified DADA 2 km (DA2) models, with the addition of forecasts from non-hydrostatic ALARO 2 km (AL2) model. AL8 and DA2 forecasts were initialized daily at 0000 UTC and driven with the ARPEGE global model forecasts through the 72-hourly forecasting range with the 3-hourly interval of data availability, while AL2 model was initialized from 0600 UTC AL8 forecasts and run through the 24-hours forecast range with the 1-hourly interval of data availability.

The results of RMSE decomposition showed that RMSE values are largest at bora dominated coastal stations (bo) and significantly decrease at coastal stations with significant portion of thermally driven flows (th). RMSE values are smallest within third group (hi), composed of highland valley and mountain foothill stations. As RMSE is generally proportional to wind speed this feature is quite expected, as well as the fact that RMSE is generally highest during winter and smallest in summer. Increase of ALADIN horizontal resolution significantly decreases RMSE at 'bo' group of stations, while the improved model setup (complete physics and non-hydrostatic) at higher resolution had significant effect on RMSE only at 'th' group of stations. The largest portion of RMSE errors can be attributed to phase errors (PHE), except maybe for AL8 model at bora dominated stations where bias of the mean (BM) has similar or even greater contribution. With the increase of model resolution BM and bias of the standard deviation (BSD) generally decrease, while the PHE increases.

The quantitative spectral evaluation of wind components was performed in the frequency domain. Entire spectral range was separated in the following three bands: larger than diurnal (LTD; 26 hours < T < 7 days), diurnal (DIU; 22 hours < T < 26 hours) and sub-diurnal (SUB; 6 hours < T < 22 hours). Within the evaluation procedure we consider the share of spectral power (observed or modelled) in different spectral ranges normalized by the total power (observed or modelled), as well as the ratio of modelled and observed power within individual spectral range. If the first one would be the same for both the model/observations and the second equals one, then we would have an ideal modelled spectra. In order to test the efficiency of our models in simulating observed spectra for different types of stations, we have made a scatter plot with the above mentioned two spectral features on coordinate axis (Fig. 27). If we first focus on observations and variability along x-axis, we clearly see that totally 12 stations can be classified into three groups. On the other hand, neither of the model data does not display such a difference between various groups of stations. Generally, with increasing the model horizontal resolution and then its complexity at finer resolution, the share of power within individual ranges becomes closer to observations. This is especially the case for the 'bo' group of stations and somewhat less for the others. Generally, the shares are poorly represented for 'hi' group of stations. Now we shall focus on the ratio of modeled and observed spectral power within individual spectral ranges (y-axis, Fig. 27). We can see that this ratio is mostly

underestimated by AL8 model in LTD and SUB ranges for ‘bo’ group of stations, as well as in LTD range for ‘hi’ stations. Both higher resolution models overestimate this range in all ranges and for all group of stations, i.e. their spectra are shifted upwards along y-axis, or more precisely they have more realistic share of power within individual ranges than AL8, but the total amount of power in the system is overestimated.

Finally, we have made some effort to link the results of statistical and spectral verification, i.e. we have tried to find how different contributors to RMSE affect the model ability to represent observed spectra. Preliminary results have shown that the along y-axis shift of modeled spectra (overestimation of total spectral power) is significantly related to BSD, where negative BSD is related to downward shift and positive BSD to upwards shift of modeled spectra. The correlation is very strong, and does not depend on the model resolution or type of the station. On the other hand, the model ability to represent the proper share of spectral power in different spectral ranges does not show such a strong link to any of the RMSE components, except for the ‘bo’ group of stations which is the most homogeneous of all groups. Despite similar spectral characteristics, shares of RMSE components differ for all other groups which weaken the correlation.

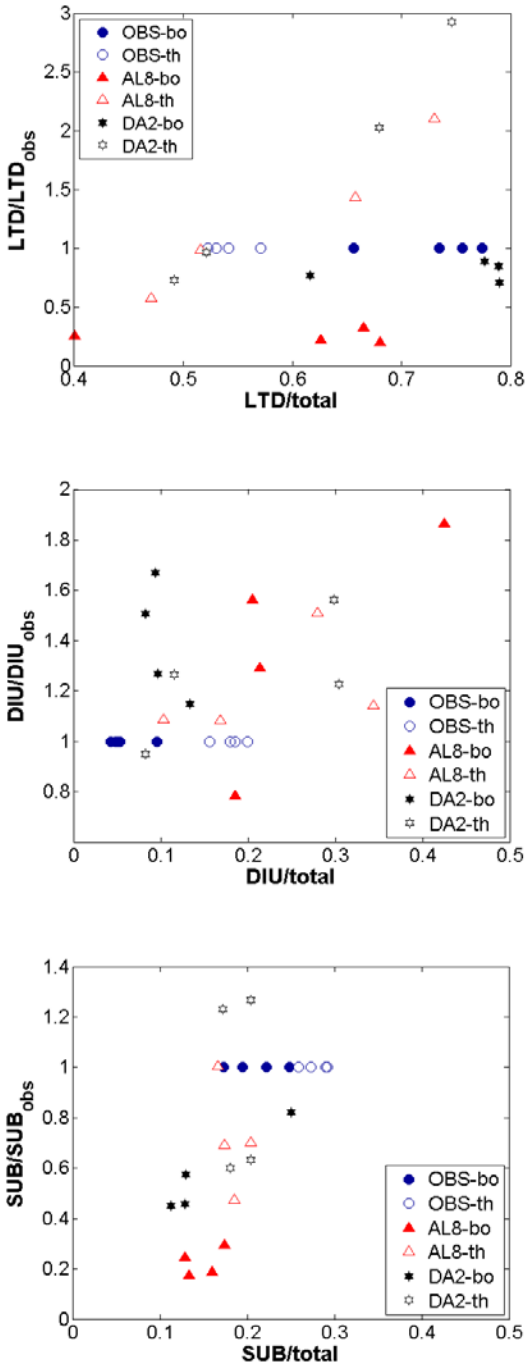

Figure 28. *The spectral power distribution of cross-mountain wind component (measured or modeled) in different spectral ranges normalized by total power (measured or modeled; x-axis) and by the observed power in the same spectral range (y-axis) at the same station.*

6. Plans for the future *(next 4 years)*

6.1 Development of the GDPFS

6.2 Planned research Activities in NWP, Nowcasting and Long-range Forecasting

According to the results of testing over a three year period in complex terrain of Croatia, the analogue-ensemble post-processing method increases the accuracy of the wind speed predictions of the current NWP operational system. Further research is needed, especially in the area of extreme winds. If the methods provides useful for extreme winds, it will be tested operationally.

6.2.1 Planned Research Activities in NWP

Improve surface conditions by using new correlation functions in surface data assimilation, test different procedures for obtaining B matrix, use 3h assimilation cycle instead of current 6h assimilation cycle, include new observations in data assimilation (MODE-S, GPS…).

Further research in post-processing methods will focus on analogue ensemble and Kalman filtering for wind speed and solar irradiance forecasting. This will include forecast uncertainty estimates derived with analogue ensemble method. It is expected that these methods will become quasi-operational in near future.

Improved representation of surface in the forecast model through improved sea surface temperature (SST) and physiographic fields (topography, roughness length, soil types).

Plans for the WWM include comparison of model output to measured data, second order wave spectrum, optimization of source terms and coupling. Data comparison between model output and measurement is fundamental to good modeling in every case. Comparison between model output and data is always possible: Altimeter estimates of sign cant wave height and wind speed can be used to compare model output on tracks. Buoys measurements can be used and radar station can measure wave height to some degree. P.A.E.M. Janssen (ECMWF) has devised a decomposition of the wave spectrum into free waves and standing waves. This decomposition has to be done at the level of data output and does not affect the model itself. The decomposition itself is very expensive computationally. But if one restricts to only station output then it is all ok. For the significant wave height, the decomposition has no effect at all. For other variables such as wave period, improvements have been reported in data comparison. Among the main terms in the equation, only the advection,

Among the main terms in the equation, only the advection, refraction and frequency shifting have a expression coming from first principle. The source terms have mostly no closed form expression and heuristic are necessary in order to get expressions for their value. Thus there is a degree of uncertainty in the coefficients used for the source term functions, mainly in the wind input source term function. The solution to that is to fit the coefficients of the source term formulation in order to get the right values.

6.2.2 Planned Research Activities in Nowcasting

Planned activities include installation of the new version of the NWC SAF software and evaluation of the products in the local environment. Additionally, MPEF GII (Global Instability Index) products will be evaluated and development of the combined forecast instability index, based on the evaluation using lightning data, is planned.

Further work on wind nowcasting and ultra-short range forecasting up to 3 hours lead time with 10-min interval is planned to finalize the research results and implement the system quasi-operationally into the ALADIN forecast system at DHMZ.

6.2.3 Planned Research Activities in Long-range Forecasting

7. Hydrological / hydraulic modelling

7.1. Introduction

DHMZ, Hydrology division is using three different hydrological models: Sava and Kupa until Sisak, European Flood Awareness System (EFAS) and WMO Flash Flood Guidance System (FFGS).

7.2. Models

7.2.1. Sava and Kupa until Sisak

We have developed our own hydrologic/hydraulic model of Sava catchment from the Slovenian border until the town of Sisak with partner Croatian Waters and DHI/Proning as consultants. It was done within period September 2014 - September 2015. The model was built within MIKE11 software (DHI). It is operational, runs regularly at hourly frequency at DHMZ on a PC, but still in a testing phase.

7.2.1.1. Equipment in use for the hydrological operational forecasting system (HOFS)

The computer used for the HOFS is a PC HP ProDesk 490 G2 MT with Intel Core i7-4790 CPU 3,6 GHz and 8 GB RAM. It runs in Win 7 Professional on 64 bit. The storage is on internal HDD of 15 GB. The model runs in MIKE11 software (DHI) and DHMZ has 2 network licenses. The hard key (dongle) for it is installed on Hydrology division's server.

7.2.1.2. Hydrological operational forecasting system (HOFS)

A combined hydrological-hydrodynamic MIKE11 model has been developed partly based on the existing hydrodynamic sub-models, existing upstream sub-models developed jointly with Agency for Environment (ARS) in Slovenia and new hydrological sub-models which have not been already modelled. After development and calibration of the MIKE11 model, the model has been upgraded to a forecasting model, which is applied in the operational flood forecasting system. The final forecasting system has been installed at DHMZ and at Croatian Waters (HV), where it is possible to run additional flood control scenarios. The forecast are issued automatically each hour for the next 4 days.

During a period of 12 months, an operational flood forecasting system has been developed for the Kupa and Upper part of Sava River to the confluence at Sisak Town, including tributaries to these two rivers. The forecasting system provides forecasts of water level and discharge on 43 river locations, for the next 4 days.

The forecasting system is synchronized with a similar Slovenian flood forecasting system at ARSO including real-time exchange of inflow forecast and online data. The HOFS is completely automated and provides a new forecast each hour with a total execution time of 5 minutes. All forecasts are disseminated to a WEB page where it is possible to monitor flood warning status for the next 4 days on a map, on charts, in tables and in reports.

The HOFS is a Cloud based forecasting system, which has been installed physically on a PC at DHMZ's premises, but can work from any location. After the forecast simulation is completed, the model behind the forecast simulation with all real-time data is made available in the cloud ready for further processing. When required, it is possible to make further analysis of the forecast, including simulation of various flood control scenarios. Provision for simulation of these scenarios has been made operational on computers at both HV and DHMZ.

The HOFS with MIKE11 is based on the real-time data received from available online hydrological and meteorological stations in Croatia, relevant online data received from Slovenia and prediction from the meteorological models ALADIN and ECMWF as shown at the Fig. 29.

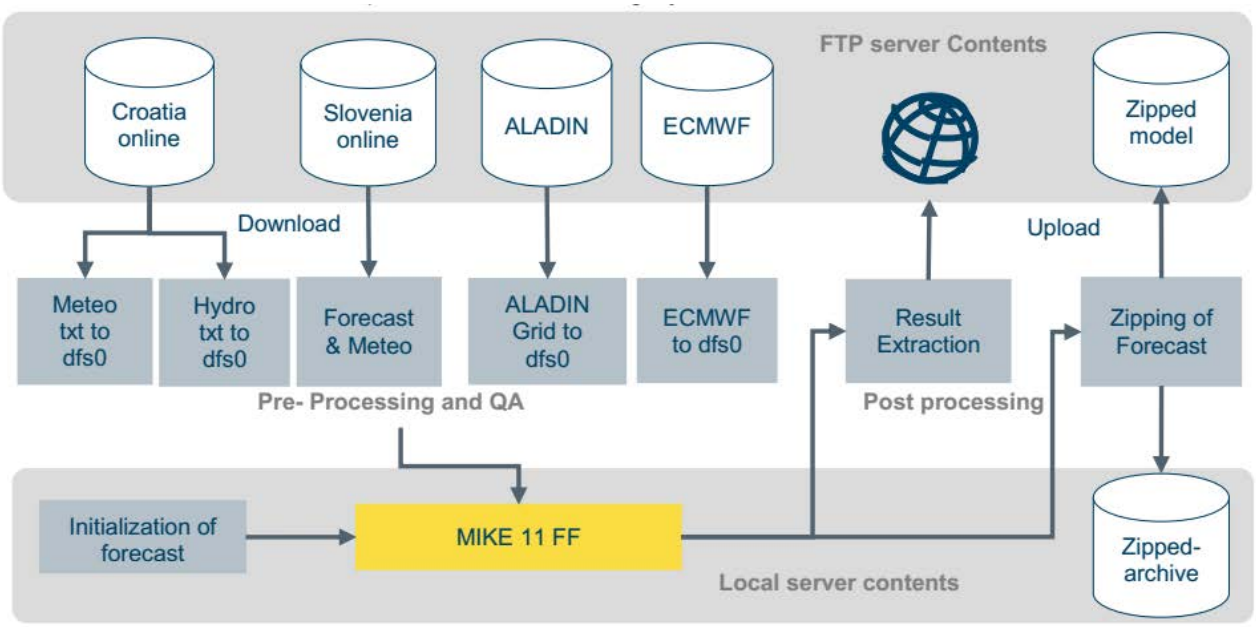

Figure 29. *Automated flood forecasting sequence (systems flowchart)*

The automated system runs each hour using the following steps:

1) Firstly, all online data required for making a flood forecast are collected on a FTP Server located at DHMZ. The online data includes data form the Hydro-Meteorological Telemetric Network (collected from DHMZ online database), online data and inflow forecast from Slovenia (prepared and uploaded by ARSO in Slovenia) and prediction from the Meteorological Models: ALADIN and ECMWF (prepared by meteorologists at DHMZ).

2) When all online data are ready on the FTP server, data are downloaded for further processing and control before the time series can be applied in MIKE11.

3) The Forecast simulation takes place as a batch job running MIKE11, initialized each hour to start a MIKE11 simulation, which is performed as a so called hot-start run using conditions form the previous simulation.

4) After the forecast simulation is completed, results are extracted and uploaded to a web page.

5) Finally, the completed model setup including time series is compressed into a zip-file and uploaded to the FTP Server, which makes it possible to run scenarios using MIKE Operations at any location. The automated system is scheduled to run each hour, and is prepared as one complete batch job which run a sequence of all jobs required in the 5 step procedure described above. The complete sequence of batch jobs (total 16 jobs) is normally executed within 5 minutes.

Results from the forecast simulation are uploaded to a Web Page as shown below in Figure 30.

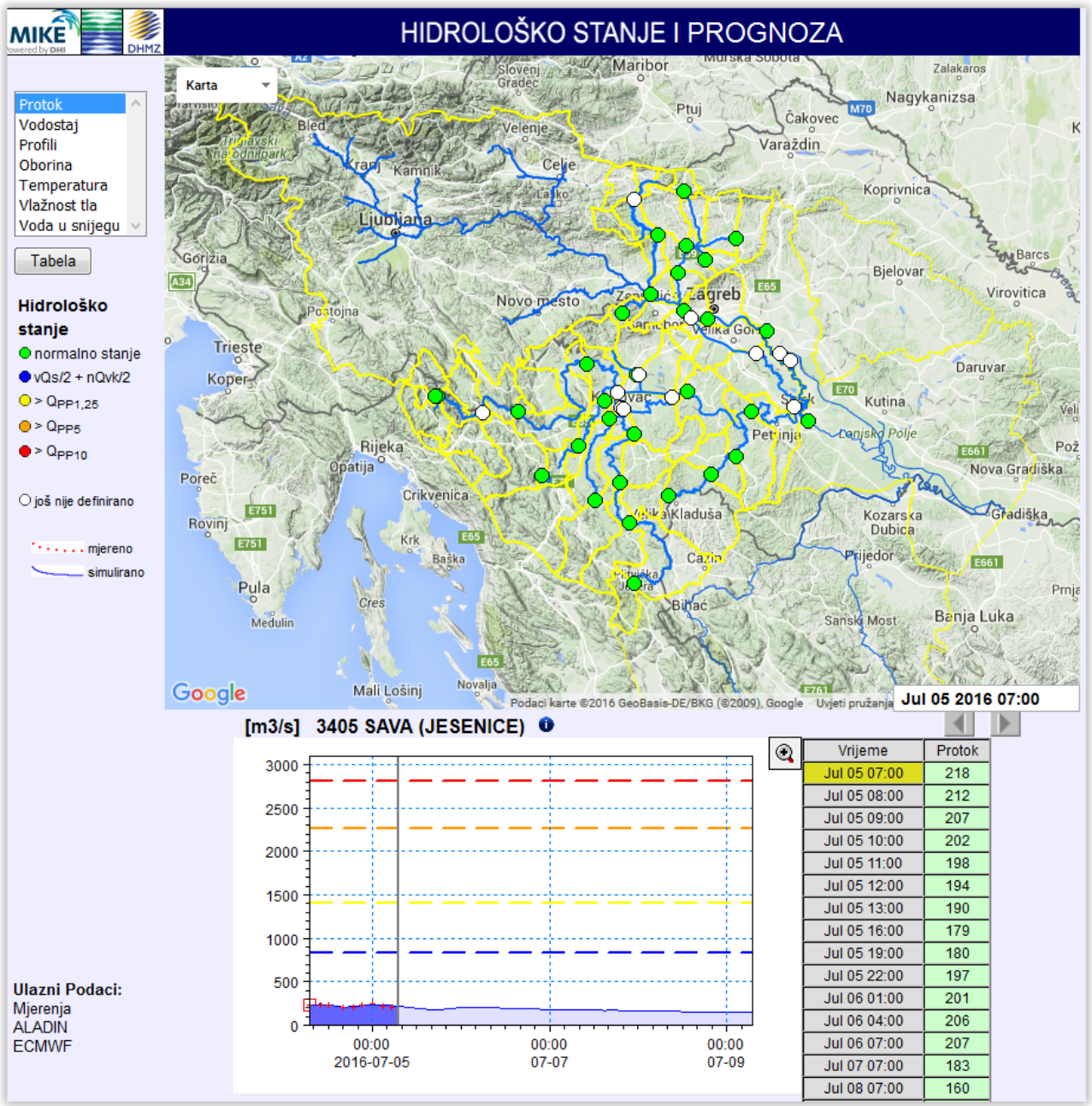

Figure 30. *Screen dump of forecasting web page for forecast disseminations*

The WEB page gives presentation of 6 data types including:

- Discharge
- Water level (also presented within a river profile)
- Precipitation
- Temperature
- Moisture content in root zone
- Snow depth (water equivalent)

Each data type has been colour coded showing warning levels (used for discharge and water levels) or coloured according to the size of values (used for other data types). Time series for each station or sub-catchment are presented on charts and tables when clicking on the map. In addition all data are presented in reports for each data type.

7.2.1.3. Development of the DHMZ's HOFS

We continue to develop the Sava HOFS downstream of Sisak to the Serbian border through the new project. A combined hydrological/hydrodynamic MIKE11 model will, as the first step, be implemented for the model extension from Sisak to the Serbian border. The extension of the model has been subdivided in three parts. The first part (Extension 1a) includes the extension from Sisak to Mačkovac in Croatia. Extension 1b covers Una and Sana Rivers, while the remaining part from Mačkovac to the Serbian border is included in Extension 2. As the next step the extended model will be upgraded to a real time flood forecasting model, which can then be applied in the HOFS.

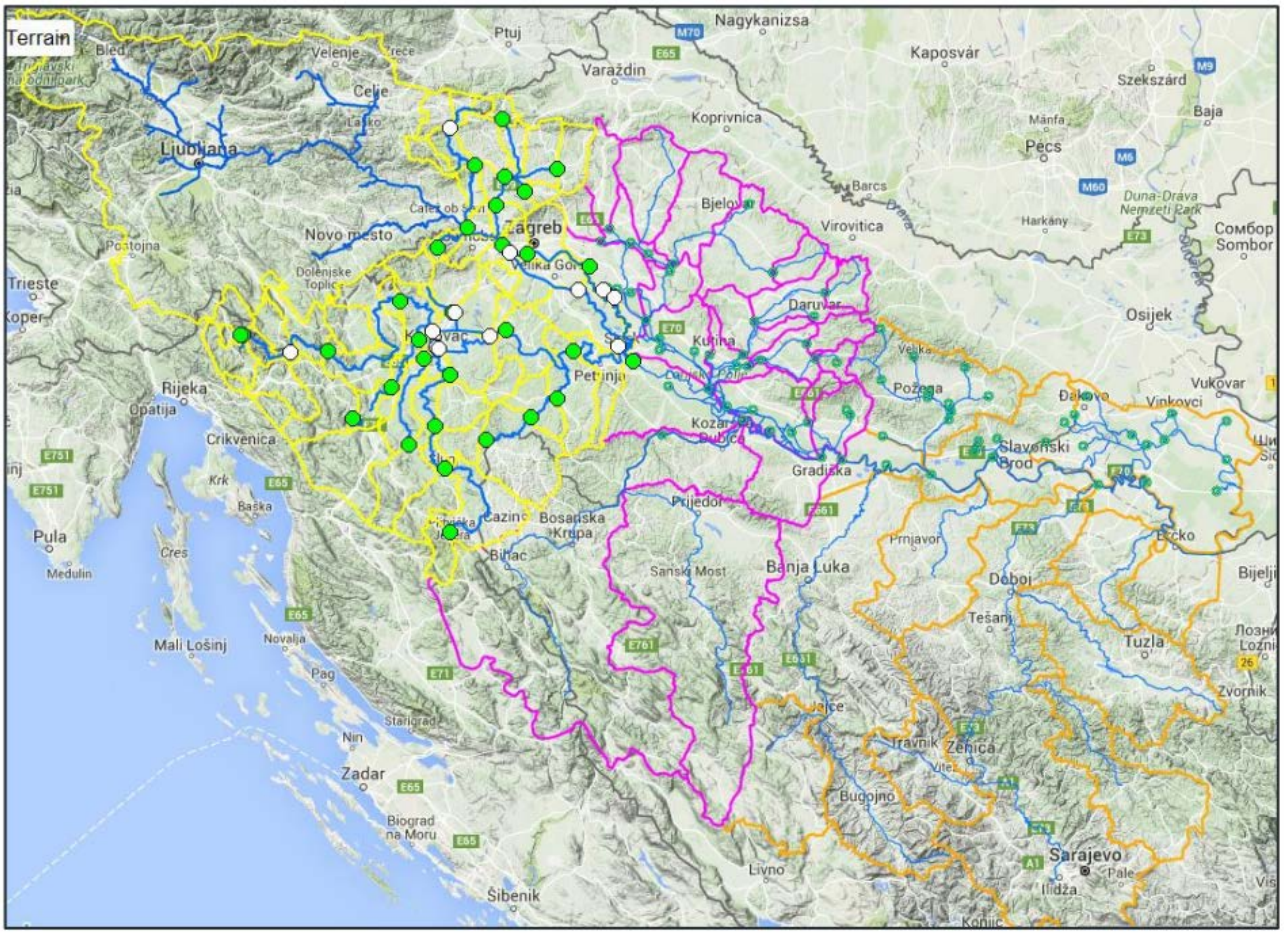

Figure 31. *Extent of the full forecasting model for the Sava River up to the Serbian border.* ***1.*** *Slovenian model (upstream yellow catchment);* ***2.*** *Sava-Kupa model (yellow sub-catchments including 43 forecast locations);* ***3.*** *First part of the model extension (pink area between Sisak and Mačkovac);* ***4.*** *Second part of the model extension (orange area, remaining part up to the Serbian border). New 76 forecasting locations in Croatia are shown as small dark green circles.*

7.2.1.4. The Sava river HOFS

During the first phase of HOFS development we covered 10533 km^2 or cca 19 % of Croatia, and during the second phase that is still in progress we'll cover 13709 km^2 or cca 24 % of country. By the end of the year 2016 we'll cover all Sava river catchment area in Croatia that is 43% of Croatian teritory. We'll have HOFS at 119 hydrological stations with 96 hours lead time.

7.2.2. European Flood Awareness System (EFAS)

From the year of 2013 DHMZ as a partner joined the EFAS and started to prepare and send data to it. It runs in ECMWF in two different models-one for fluvial (river) flooding and the second one for the flash flooding. The EFAS Partnership gives the Partner real-time access to the EFAS products through the EFAS Information System (EFAS-IS).
EFAS is the first operational European system monitoring and forecasting floods across Europe. It provides probabilistic, flood early warning information up to 10 days in advance to its partners: the National Hydrological Services and the European Response and Coordination Centre (ERCC).
The Operational EFAS consists of four centres executed by different consortia:

- **EFAS Computational** centre - European Centre for Medium-Range Weather Forecasts (UK) executes forecasts and hosts the EFAS-Information System platform
- **EFAS Dissemination** centre - Swedish Meteorological and Hydrological Institute, Rijkswaterstaat (NL) and Slovak Hydro-Meteorological Institute analyse EFAS on a daily basis and disseminate information to the partners and the ERCC
- **EFAS Hydrological data collection** centre - REDIAM (ES) and ELIMCO (ES) collect historic and realtime discharge and water level data across Europe
- **EFAS Meteorological data collection** centre – KISTERS AG and Deutscher Wetterdienst collect historic and realtime meteorological data across Europe.

EFAS is an operational service under the umbrella of the Copernicus emergency management service and is fully operational since October 2012.

Ensemble Prediction Systems – key to longer flood warning times

Most hydrological services rely either on observations only or on short-term deterministic rainfall forecasts of up to two days or less because the high degree of uncertainty in weather forecasts at longer lead times. Since these uncertainties are also unpredictable, they render the results unreliable and therefore not useful for decision making. Since the last 10 years, however, the hydrological community is looking increasingly at the use of ensemble prediction systems (EPS) instead of single (deterministic) forecasts for flood warning times beyond 48 hours. EPS have already become an integral part of operational weather forecasts over the past years. They are designed to give a measure of the predictability of the weather and uncertainty in the model solution for lead times up to two weeks which would be considered well outside the range of predictability for deterministic models. The trend for implementing hydrological ensemble prediction systems in operational flood forecasting centres can clearly be seen in Europe. EFAS uses multiple weather forecasts and EPS as input. Its forecasts are based on two deterministic, medium-range forecasts from the European Centre for Medium-Range Weather Forecasts (ECMWF) and the German Weather Service (DWD), (and thus different models) and on two sets of EPS: One from ECMWF which covers the medium-range up to 15 days globally (with a spatial resolution of ~30 km and 51 members, and one from the Consortium for Small-scale Modelling (COSMO), a limited area model EPS covering most of Europe with a shorter range up to 5 days (with a spatial resolution of 7 km and 16 members). The reason for using the shorter term EPS is to enhance the spread of EPS within the first few days and to have finer grid information in particular for mountainous areas. This allows to better identifying the location of the floods within the river basin. In a case study it has been demonstrated that using the eight global medium-range EPS available worldwide can provide a higher reliability for the results, but is computationally intensive.

LISFLOOD – the hydrological model for EFAS

The hydrological model used for EFAS is LISFLOOD. The model is a hybrid between a conceptual and a physical rainfall-runoff model combined with a routing module in the river channel.

LISFLOOD has been specifically designed for large river catchments. A particular feature of LISFLOOD is its strong use of advanced Geographical Information System (GIS), in particular as a dynamic modelling framework.

Processes simulated include:

- Interception of rainfall by vegetation (Int)
- Evaporation of intercepted water (EWint)
- Leaf drainage (Dint)
- Snow accumulation and snowmelt
- Direct evaporation from the soil surface (ESa)
- Water uptake and transpiration by plants (Ta)
- Infiltration (INFact)
- Preferential flow through macro-pores (Dpref,gw)
- Surface runoff (Rs)
- Gravity-driven vertical flow within (D1,2) and out of (D2,gw) the soil
- Rapid (Quz) and slow (Qlz) groundwater runoff
- Channel routing using kinematic (and optionally dynamic) wave

Reducing false alarms – threshold exceedance and persistence

EFAS is providing information to the national hydrological services only when there is a danger that critical flood levels might be exceeded. In EFAS, the critical thresholds are needed at every grid point and therefore cannot be derived from observations. Instead, based on observed meteorological data, long term discharge time series are calculated at each grid with the same LISFLOOD model parameterisation that is set up in the forecasting system. From these long-term simulations return periods are estimated – currently the 1, 2, 5 and 20-year return periods. All flood forecasts are compared against these thresholds – at every pixel – and the threshold exceedance calculated. Only when critical thresholds are exceeded persistently over several forecasts, information at these locations is produced, e.g. in the form of colour-coded overview maps or time series information at control points. The persistence criteria has been introduced to reduce the number of false alarms and focus on large fluvial floods caused mainly by widespread severe precipitation, combined rainfall with snow-melting or prolonged rainfalls of medium intensity.

Verification

Forecast verification is important to understand the strength and weaknesses of the system and to build confidence in its results. For EFAS two types of verifications are applied. The first one is event-based – for each flood alert the hit, false alarm and misses are assessed. If a flood alert has been sent but no flooding was observed, a false alarm is counted. If somewhere in the basin flooding has been report, a hit is counted. If flooding has been reported for which an alert was not sent (even if the system itself simulated an event), a missed event is counted. The events are assessed through feedback reports and media throughout the year and reported during the EFAS annual meeting. In addition to the event-based verification, also skill scores are computed including Brier Skill Score, Root Mean Square Error, Nash Sutcliffe efficiency, continuous rank probability score, etc. These are reported regularly in the EFAS bulletins and in publications. More on skill scores can be found on HEPEX. The specific verification tool box for hydrological ensemble prediction has also been tested for EFAS.

7.2.3. Flash Flood Guidance System (FFGS)

At the XV congress of the WMO in 2007, it was decided to establish a Flash Flood Guidance System program worldwide. Flash Flood Guidance System was developed and is being implemented by HRC (Hydrologic Research Center, San Diego, USA) and financed by USAID/OFDA in collaboration with NOAA/WMO.

Flash flood global coverage concept plan is to eventually establish a series of regional centers, which will provide flash flood related products and support services to their respective regional participating country National Meteorological and Hydrologic Services (NMHSs). Using those products, NMHSs can provide flash flood watches and warnings to their own national agencies like emergency management authorities, municipalities, and water resources agencies. Meeting for the establishment of a Flash Flood Guidance System for South East Europe (SEE) was held in Ankara, Turkey on 22-24 January 2013. Croatia, Serbia, Slovenia, Romania, Bosnia-Herzegovina, Macedonia, Moldova, Albania and Montenegro as well as Turkey, WMO, HRC, and OFDA delegates participated. It was agreed to establish South East Europe Flash Flood Guidance System (SEEFFGS) making Turkey the regional center.

DHMZ started to prepare and sent data (digital elevation model, flash flood sub basin delineation, soil and land cover data, historical meteorological and hydrological data) for the establishing SEEFFGS from the year of 2014. The FFGS for Croatia is operational from September 2015, after completed e-Learning Course Certification and additional Specialized Training at HRC. It runs regularly at HRC in San Diego and it will move to Regional center in Turkey, Ankara. DHMZ has real time access to the FFGS through its web page (Dashboard console).

Dashboard console has four main toolbars – including Real Time Data Download and Inventory Status, Real Time Data Processing Status, Computational Server Status and Dissemination Server Status. Even though the Dashboard is designed primarily for system administrators, it also has four different products displayed in windows at the top of the console including Global Hydrometeor Estimator (GHE), Meteorological Station Data Reception Status, Average Soil Moisture (ASM) and Forecast Mean Areal Precipitation (FMAP). At the bottom of the dashboard, you can click on a given country and the products displayed in the dashboard will be for that country only. Also, at the bottom there is a link for the product console. Clicking on this link will take you to the forecaster interface (Fig. 32).

Interface: The products are presented as thumbnails on the interface; clicking on the thumbnail provides a larger image. The main features of the console are as follows:

1. At the top of the main page, products, date and time selection toolbars are provided. A user can use this toolbar to navigate to different dates and times and to display products for selected countries.
2. SEEFFG main products are listed consisting MWGHE (Micro Wave adjusted Global Hydrometeor Estimator) precipitation, GHE (Global Hydrometeor Estimator) satellite precipitation estimates, Gauge MAP (Gauge Mean Areal Precipitation based on gauge data only), Merged MAP (Merged Mean Areal Precipitation), ASM (Average Soil Moisture), FFG (Flash Flood Guidance), IFFT (Imminent Flash Flood Threat), PFFT (Persistence Flash Flood Threat), ALADIN Forecast, FMAP (Forecast Mean Areal Precipitation), FFFT (Forecast Flash Flood Threat).
3. On the left side of the FFGS Products, the time intervals (1, 3, 6, and 24 hour) are displayed.
4. Below the FFGS Products, selected surface meteorological observations (Synoptic Stations) from the member states and disseminated through the WMO GTS (Global Telecommunication System) are displayed.

5. Snow products including Gauged MAT (Mean Areal Temperature), Latest IMS SCA (Snow Coverage Area), SWE (Snow Water Equivalent), and MELT are displayed at the bottom of the main interface.
6. At the bottom of the interface page, products description and system monitoring tools are listed consisting of products description, processing logs, server monitor, static resources and a link back to Dashboard.

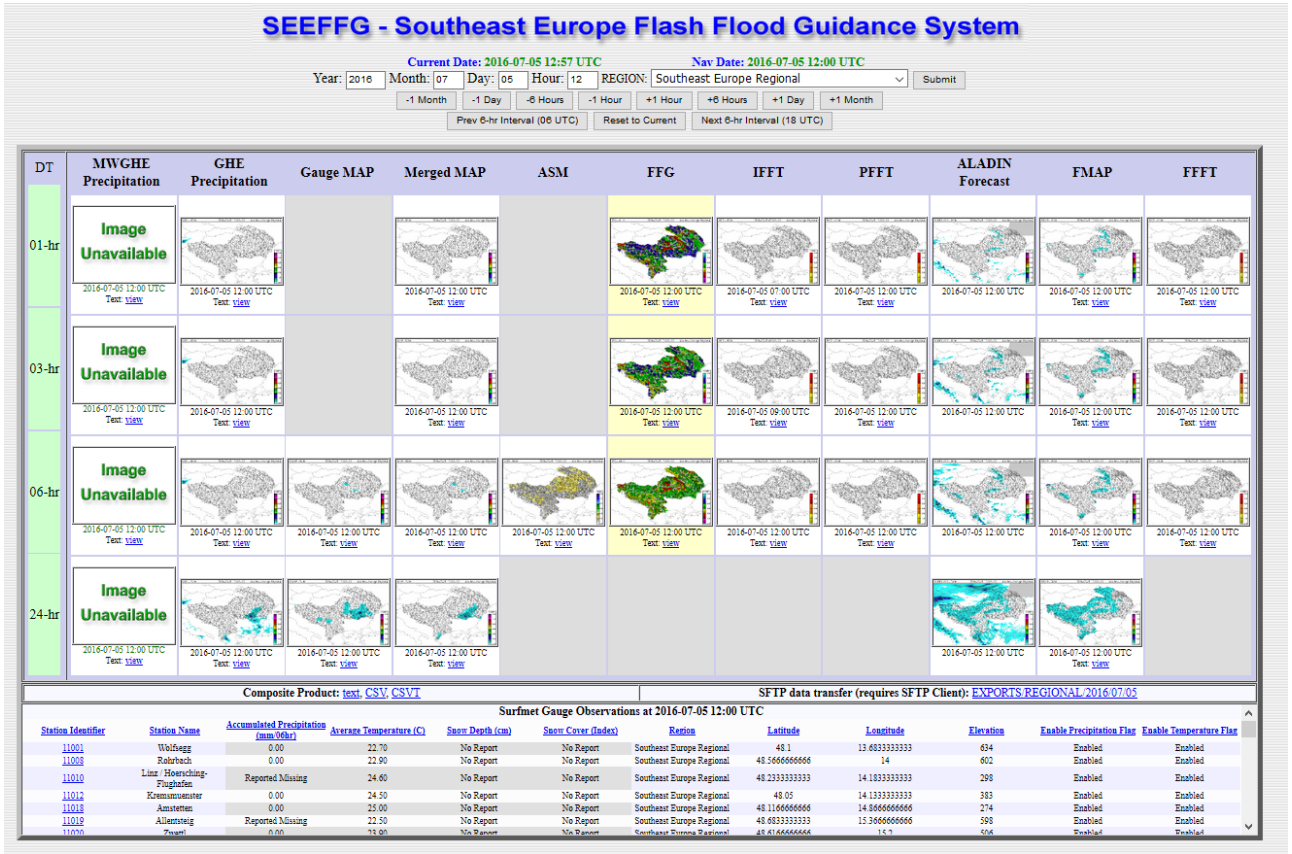

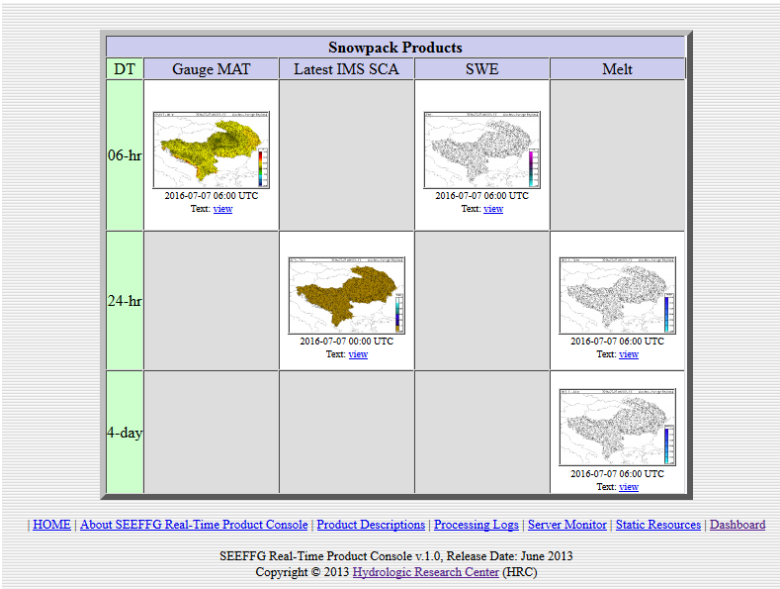

Figure 32. *SEEFFGS Forecasters interface.*

The SEEFFG forecaster product console displays product for each sub-basins but does not provide any geographical information like cities, roads, border, etc. Because Flash Flood forecasters would like to see not only products but also additional layers that are displayed with the products so that precise event locations can be determined. Thus, DHMZ hydrological forecasters use GIS software before issuing flash flood warnings. For this purpose, Turkish Meteorological Service (regional center) uses GIS sever which will also be available for all member state forecasters.

Verification of flash flood events are not easy task but very important to evaluate the performances of the FFG system. DHMZ collects flash flood event reports (from National Protection and Rescue Directorate and press) to create maps and contingency tables.

8. References

Bajić, A., Ivatek-Šahdan, S., Žibrat, Z. (2008): ANEMO-ALARM iskustva operativne primjene prognoze smjera i brzine vjetra. GIU Hrvatski cestar. 109-114

Boloni G. and K. Horvath, 2010: Diagnosis and tuning of background error statistics in a variational data assimilation system**.** *Idojaras*, 114, 1-19.

Branković, Č., I. Güttler, M. Gajić-Čapka (2013): Evaluating climate change at the Croatian Adriatic from observations and regional climate models' simulations. *Clim. Dyn.*, 41, 2353–2373

Catry B., Geleyn J.-F., Tudor M., Bénard P. and Trojakova A. (2007): Flux conservative thermodynamic equations in a mass-weighted framework. Tellus 59A, pp 71–79.

Dee, D.P. and Coauthors (2011): The ERA-Interim reanalysis: configuration and performance of the data assimilation system. *Q. J. R. Meteorol. Soc.*, 137, 553–597

Delle Monache, L., Eckel, T., Rife, D., Nagarajan, B., 2013: Probabilistic weather prediction with an analog ensemble. Monthly Weather Review 141, 3498-3516.

H. Davies, 1983: Limitations of some common lateral boundary schemesused in regional NWP models, Mon.Wea.Review., 111, 1002-1012

Geleyn J.-F. (1988): Interpolation of wind, temperature and humidity values from model levels to the height of measurement. Tellus, 40A, pp.347–351.

Geleyn J.-F. and Hollingsworth A (1979): An economical analytical method for the computation of the interaction between scattering and line absorption of radiation. Beitr Phys Atmos 52:1–16.

Geleyn J.-F., Benard P. and Fournier, R. (2005a): A general-purpose extension of the Malkmus band-model average equivalent width to the case of the Voigt line profile. Quart. J. Roy. Meteor. Soc. 131:2757–2768

Geleyn J.-F., Fournier R., Hello G., Pristov N. (2005b): A new 'bracketing' technique for a flexible and economical computation of thermal radiative fluxes, scattering effects included, on the basis the Net Exchanged Rate (NER) formalism. WGNE Blue Book

Geleyn J.-F., Vana F., Cedilnik J., Tudor M. and Catry B. (2006): An intermediate solution between diagnostic exchange coefficients and prognostic TKE methods for vertical turbulent transport. WGNE Blue Book

Geleyn J.-F., Catry B., Bouteloup Y. and Brožkova, R. (2008): A statistical approach for sedimentation inside a microphysical precipitation scheme. Tellus 60A,649–662

Gerard, L. (2007): An integrated package for subgrid convection, clouds and precipitation compatible with the meso gamma scales. Quart. J. Roy. Meteor. Soc., 133, 711–730.

Gerard, L. and Geleyn, J.-F. (2005): Evolution of a subgrid deep convection parameterization in a limited area model with increasing resolution. Quart. J. Roy. Meteor. Soc., 131, 2293–2312.

Gerard, L., Piriou, J.-M., Brožková, R., Geleyn, J.-F. and Banciu, D. (2009): Cloud and Precipitation Parameterization in a Meso-Gamma-Scale Operational Weather Prediction Model. Mon. Wea. Rev., 137, 3960–3977.

Giard, D. and Bazile, E. (2000): Implementation of a new assimilation scheme for soil and surface variables in a global NWP model. Mon. Wea. Rev. 128, 997-1015.

Giorgi, F., E. Coppola, F. Solmon, L. Mariotti, M.B. Sylla, X. Bi, N. Elguindi, G.T. Diro, V. Nair, G. Giuliani, S. Cozzini, I. Güttler, T.A. O'Brien, A.B. Tawfik, A. Shalaby, A.S. Zakey, A.L. Steiner, F. Stordal, L.C. Sloan, C. Brankovic (2012): RegCM4: Model description and preliminary tests over multiple CORDEX domains. *Clim. Res.*, 52, 7–29

Güttler, I., Č. Branković, L. Srnec, M. Patarčić (2014): The impact of boundary forcing on RegCM4.2 surface energy budget. *Climatic Change*, 125, 67–78

Haiden, T., A. Kann, C. Wittmann, G. Pistotnik, B. Bica, Gruber, C. (2011): The Integrated Nowcasting through Comprehensive Analysis (INCA) System and Its Validation over the Eastern Alpine Region. Wea.Forecasting, 26, 166 183.

Haylock, M.R., N. Hofstra, A.M.G. Klein Tank, E.J. Klok, P.D. Jones and M. New (2008): A European daily high-resolution gridded dataset of surface temperature and precipitation. *J. Geophys. Res (Atmospheres)*, 113, D20119, doi:10.1029/2008JD10201

Hazeleger, W. and Coauthors (2010). EC-Earth: A seamless Earth-system prediction approach in action *Bull. Amer. Meteor. Soc.*, 91, 1357-1363

Horvath, K., D. Koracin, R. K. Vellore, J. Jiang, and R. Belu, 2012: Sub-kilometer dynamical downscaling of near surface winds in complex terrain using WRF and MM5 mesoscale models. J. Geophys. Res., 117, D11111, 19pp., doi:10.1029/2012JD017432.

Horvath, K., Bajić, A., & Ivatek-Šahdan, S. (2011): Dynamical Downscaling of Wind Speed in Complex Terrain Prone To Bora-Type Flows. J. Appl. Meteor. Climatol., 50, 1676–1691.

Horvath, K., Ivatek-Šahdan, S., Ivančan-Picek, B. and Grubišić, V. (2009): Evolution and structure of two severe cyclonic bora events: contrast between the northern and southern Adriatic. Weather and forecasting 24, 946-964.

Iršić, M., Predoš, A., Zgonc, T., Strelec Mahović, N. (2004): CEI Nowcasting tools based on remote sensing data in Croatia and Slovenia. Proceedings - 2004 EUMETSAT Meteorological Satellite Conference, Prague, Czech Republic, 31 May - 04 June 2004.

Ivatek-Šahdan, S. & Ivančan-Picek, B. (2006): Effects of different initial and boundary conditions in ALADIN/HR simulations during MAP IOPs. Meteorol. Z. 15, 187–197.

Ivatek-Šahdan, S. & Tudor M. (2004): Use of high-resolution dynamical adaptation in operational suite and research impact studies. Meteorol Z 13(2):1–10

Janeković, I. Mihanović, H. Vilibić, I. Tudor, M. (2014) Extreme cooling and dense water formation estimates in open and coastal regions of the Adriatic Sea during the winter of 2012. Journal of geophysical research : oceans. 119 , 5; 3200-3218.

Jeričević, A., Kraljević, L., Vidič, S., and Tarrasón, L. (2007): Project description: High resolution environmental modelling and evaluation programme for Croatia (EMEP4HR), Geofizika, 24 (2), 137-143, available form http://geofizika-journal.gfz.hr/vol24.htm.

Jeričević, Amela; Večenaj, Željko (2009): Improvement of vertical diffusion analytic schemes under stable atmospheric conditions. Boundary - Layer Meteorology. 131, 2; 293-307.
Jeričević, Amela; Kraljević, Lukša; Grisogono, Branko; Fagerli, Hilde; Večenaj, Željko (2012): Parameterization of vertical diffusion and the atmospheric boundary layer height determination in the EMEP model. Atmospheric chemistry and physics. 10, 2; 341-364.
Jeričević, Amela; Fagerli, Hilde; Grisogono, Branko (2011): Exploring the properties of local and non-local vertical diffusion schemes in the EMEP model using 222Rn data. International journal of environment and pollution. (in press)
Kalinić, H. Mihanović, H. Cosoli, S. Tudor, M. Vilibić, I. (2016) Predicting ocean surface currents using numerical weather prediction model and Kohonen neural network: a northern Adriatic study. // Neural Computing and Applications. 11(in press)
Kessler, E., 1969. On distribution and continuity of water substance in atmospheric circulations. Meteorol Monogr Am Meteorol Soc 10(32):84.
Kraljević, L., Belušić, D., Bencetić Klaić, Z., Bennedictow, A., Fagerli, H., Grisogono, B., Jeričević, A., Mihajlović, D., Špoler Čanić, K., Tarrasón, L., Valiyaveetil, S., Vešligaj, D., and Vidič, S. (2008): Application of EMEP Unified model on regional scale – EMEP4HR, Croat. Meteorol. J., 43, Proceedings from a 12 HARMO conference Part 1: Oral Presentations, /Đuričić, Vesna (Ed.), Zagreb, 151-151, available from http://www.harmo.org/Conferences/Proceedings/Cavtat/topicIndex.asp?topicID=0.
Lu, C., Yuan, H., Schwartz, B. E., Benjamin, S.G:, 2007: Short-Range Numerical Weather Prediction Using Time Lagged Ensembles. Weather and Forecasting, 22, 580-595.
Mikuš, P., Bedka, K., Strelec Mahović, N. (2011): Comparison and validation of satellite-based overshooting top detection methods. Proceedings - 6th European Conference on Severe Storms (ECSS 2011), Palma de Mallorca, Spain, 03-07 October 2011.
Mikuš, P., Strelec Mahović, N. (2011): Correlating overshooting tops and severe weather. Proceedings - 6th European Conference on Severe Storms (ECSS 2011), Palma de Mallorca, Spain, 03-07 October 2011.
MZOIP (2014) Sixth National Communication and First Biennial Report of the Republic of Croatia under the United Nation Framework Convention on the Climate Change. Republic of Croatia Ministry of Environmental and Nature Protection (MZOIP), Zagreb, pp 247

Patarčić, M. and Branković, Č. (2012): Skill of 2-m temperature seasonal forecasts over Europe in ECMWF and RegCM models. Monthly Weather Review 140, 1326-1346.
Patarčić, M., M. Gajić-Čapka, K. Cindrić, Č. Branković (2014) Recent and near-future changes in precipitation-extreme indices over the Croatian Adriatic coast. *Climate Research*, 61:157-176

Solazzo, E.; Roberto, Bianconi; Robert, Vautard; K. Wyat, Appel; Bertrand, Bessagnet; Jørgen, Brandt; Jesper H., Christensen; Charles, Chemel; Isabelle, Coll15, Hugo, Denier van der Gon; Joana, Ferreira; Renate, Forkel; Xavier, V. Francis; George, Grell; Paola, Grossi; Ayoe B., Hansen; Jeričević, Amela; Lukša, Kraljević; Ana Isabel, Miranda; Michael D., Moran; Uarporn, Nopmongco; Guido, Pirovano; Marje, Prank; Angelo, Riccio; Karine N., Sartelet; Martijn, Schaap; Jeremy D., Silver; Ranjeet S., Sokhi; Julius, Vira; Johannes, Werhahn; Ralf, Wolke; Greg, Yarwood; Junhua, Zhang; S.Trivikrama, Rao; StefanoGalmarini (2011): Model evaluation and ensemble modelling of surface level ozone in Europe and North America in the context of AQMEII. Atmospheric environment (1994). (in print)
Srnec, L., K. Cindrić, I. Güttler, Č. Branković (2014) Simulation of extremely hot events in Croatia with RegCM4, 20th International Congress of Biometeorology, Cleveland, OHIO, USA, 28.09.-2.10.2014.

Stanešić, A. (2011). Assimilation system at DHMZ: Development and first verification results. Cro. Met. J. 44/45, 3-17.
Strelec Mahović, N. (2005): Operational use of Meteosat-8 SEVIRI data and derived nowcasting products. Proceedings - 2005 EUMETSAT Meteorological Satellite Conference, Dubrovnik, Croatia, 19-23 September 2005.
Strelec Mahović, N. and Zeiner, B. (2009): Application of Meteosat SEVIRI channel difference 0.6 μm - 1.6 μm in convective cells detection. Atmos. res. 93, 1-3, 270-276
Strelec Mahović, N., Mikuš, P. (2011): Correlating locations of the overshooting tops with the occurrence of severe weather on the ground. Proceedings - 2011 EUMETSAT Meteorological Satellite Conference, Oslo, Norway, 05-09 September 2011.
Telišman Prtenjak, Maja; Jeričević, Amela; Kraljević, Lukša; Herceg Bulić, Ivana; Nitis, Theodoros; Bencetić Klaić, Zvjezdana (2009): Exploring atmospheric boundary layer characteristics in a severe SO2 episode in the north-eastern Adriatic. Atmospheric chemistry and physics. 9, 13; 4467-4483.
Tudor M. (2010): Impact of horizontal diffusion, radiation and cloudiness parameterization schemes on fog forecasting in valleys. Met. Atm. Phy. Vol.108, pp. 57-70.
Tudor, M. (2011): The meteorological aspects of the DART field experiment and preliminary results. Cro. Met. J. 44/45, 31-46.
Tudor, M. and Ivatek-Šahdan, S. (2002): The MAP-IOP 15 case study. Cro. Met. J. 37, 1-14.
Tudor, M. and Ivatek-Šahdan, S. (2010): The case study of bura of 1st and 3rd February 2007, Meteorol. Z., 19, pp. 453-466.
Tudor, M., Termonia, P., (2010): Alternative formulations for incorporating lateral boundary data into limited-area models. Mon. Wea. Rev. 138, pp. 2867-2882.
Tudor, M., 2013. A test of numerical instability and stiffness in the parametrizations of the ARPÉGE and ALADIN models. Geoscientific model development, 6, 901-913.
Tudor, M., 2015. Methods for automatized detection of rapid changes in lateral boundary condition fields for NWP limited area models. Geoscientific Model Development. 8, 2627-2643.
Tudor, M. Stanešić, A. Ivatek-Šahdan, S. Hrastinski, M. Odak Plenković, I. Horvath, K. Bajić, A. Kovačić, T.(2015a) Changes in the ALADIN operational suite in Croatia in the period 2011-2015. Cro. Meteorol. Jour. 50, 71-89.
Tudor, M. Stanešić, A. Ivatek-Šahdan, S. Hrastinski, M. Odak Plenković, I. Horvath, K. Bajić, A. Kovačić, T.(2015b) Operational validation and verification of ALADIN forecast in Meteorological and Hydrological Service of Croatia. Cro. Meteorol. Jour 50, 47-70.
Váňa F., Bénard P., Geleyn J.-F., Simon A. & Seity Y. (2008): Semi-Lagrangian advection scheme with controlled damping–an alternative way to nonlinear horizontal diffusion in a numerical weather prediction model. Quart. J. Roy. Meteor. Soc, Vol.134, pp. 523–537.
Van der Linden P, Mitchell JFB (eds) (2009) ENSEMBLES: climate change and its impacts: summary of research and results from the ENSEMBLES project. Met Office Hadley Centre, FitzRoy Road, Exeter EX1 3 PB, UK, p 160
Vautard, Robert; Moran, Michael D.; Solazzo, Efisio; Gilliam, Robert C.; Matthias, Volker; Bianconi, Roberto; Chemel, Charles; Ferreira, Joana; Geyer, Beate; Hansen, Ayoe B.; Jeričević, Amela; Prank, Marje; Segers, Arjo; Silver, Jeremy D.; Werhahn, Johannes; Wolke, Ralf; Rao, S.T.; Galmarini, Stefano (2011).
Evaluation of the meteorological forcing used for the Air Quality Model Evaluation International Initiative (AQMEII) air quality simulations. Atmospheric environment (1994). (in press).
Vilibić, I. Šepić, J. Mihanović, H. Kalinić, H. Cosoli, S. Janeković, I. Žagar, N. Jesenko, B. Tudor, M. Dadić, V. Ivanković, D. (2016a) Self-Organizing Maps-based ocean currents forecasting system. Scientific Reports. 6 ()

Vilibić, I. Kalinić, H. Mihanović, H. Cosoli, S. Tudor, M. Žagar, N. Jesenko, B. (2016b) Sensitivity of HF radar-derived surface current self-organizing maps to various processing procedures and mesoscale wind forcing. Computational geosciences. 20, 115-131.

Wang, Y., Bellus, M., Wittmann, C., Steinheimer, M., Weidle, F., Kann, A., Ivatek-Šahdan, S., Tian, W., Ma, X., Tascu, S., Bazile, E. (2011): The Central European limited-area ensemble forecasting system: ALADIN-LAEF. Quart. J. Roy. Meteor. Soc 137, 483-502.

Vautard, R., A. Gobiet, D. Jacob, M. Belda, A. Colette, M. Déqué, J. Fernández, M. Garica-Díez, K. Goergen, I. Güttler, T. Halenka, T. Karakostas, E. Katragkou, K. Keuler, S. Kotlarski, S. Mayer, G. Nikulin, M. Patarčić, J. Scinocca, S. Sobolowski, M. Suklitsch, C. Teichmann, E. van Meijgaard, K. Warrach-Sagi, V. Wulfmeyer, P. Yiou (2013): The simulation of European heat waves from an ensemble of regional climate models within the EURO-CORDEX project. *Clim. Dyn*., 41, 2555–2575

Wilks, D. S. (2006.): Statistical methods in the atmospheric sciences. Second Edition. Academic Press, London.

Žagar, M. and J. Rakovec, (1999): Small-scale surface wind prediction using dynamic adaptation. Tellus 51, 489-504.